Contents

List of Figures

Introduction

Minimal surfaces in hyperbolic space have been studied by several authors. The surfaces have many similarities with Euclidean minimal surfaces but they differ in their behavior at infinity. Complete minimal surfaces in $\mathbf{R}^3$ of finite total curvature are by a theorem of Osserman conformally equivalent to compact punctured Riemann surfaces. In H^3 the underlying complex structure has much more freedom. For example, on all surfaces which we discuss later we may vary continuously the infinite part of the boundary while keeping the finite part fixed, and our surfaces would stay complete and embedded.

The initial purpose of our work has been to study non-compact minimal surfaces in H^3 whose boundary consists of a finite part in H^3 and an infinite part on the asymptotic sphere S^∞ of H^3. This is a delicate problem since for example the hyperbolic minimal surface equation for graphs in the upper halfspace model becomes degenerate when approaching the complex plane in that model. Since standard elliptic theory does not apply directly we use additional geometric arguments in our study. This is possible since the equation becomes degenerate only for technical reasons. For example, by a result of Hardt and Lin every area-minimizing minimal surface with C^1 boundary on S^∞ intersects the sphere orthogonally and is regular, but the gradient of a corresponding graph would become unbounded.

The main results of this work consider four different topics:

- By using geometric arguments we prove new C^0 and C^1 a priori estimates for hyperbolic minimal surfaces in chapters (3) and (4). We derive a Hyperbolic Four Point Condition and use it to prove our main gradient estimates in theorems (18) and (19).

- In chapter (5) we review at first some known existence theorems for boundary contours lying completely in infinity or completely in H^3. Then we prove our new existence theorem (29) for Plateau problems with boundary contours lying in part in H^3 and in part on the asymptotic sphere S^∞. This is the first existence proof for such mixed contours, it relies on our previously derived estimates. In some sense the theorem is a generalization of the Euclidean existence theorem of Jenkins and Serrin.

- A new comparison theorem (37) for planar hyperbolic curves will be proved in chapter (6). We use information about the turning angle of a curve normal against a parallel translated vector to estimate the relative position of the two normal geodesics through start and end point of the curve. This theorem has its own interest, but we will intensively use it in our example section.

- Finally in chapters (7) and (8), we apply the previous results to prove existence of new complete embedded minimal surfaces in H^3. Many examples generalize minimal surfaces from $\mathbf{R}^3$ and thereby develop new properties. We use essentially the existence theorem (29) and the comparison theorem (37) to control our constructions.

In spite of the mentioned hierarchy we tried to keep the different chapters self-contained since they have their own interest. Finally, we give in chapter (9) a short introduction to the new minimization algorithm of Pinkall and Polthier, which we used to compute the accompanying pictures of minimal surfaces. In chapters (1) and (2) we recall properties of hyperbolic space and minimal surface theory, and prove some elementary tools we use through our work.

I would like to thank my advisor Prof. Dr. Hermann Karcher for inspiring discussions and valuable advice. He supported me through all parts of my studies and focused my interest on minimal surfaces. It was always a pleasure to work with him. Also I am grateful to the Sonderforschungsbereich 256, especially Prof. Dr. Stefan Hildebrandt, for continuous support.

Chapter 1

Preliminary Remarks on Hyperbolic Space

Hyperbolic space H^n is the complete simply connected spaceform of dimension n with constant curvature -1. This space is sometimes called Lobachevsky space in the literature, after one of the three mathematicians Bolyai, Gauss and Lobachevsky who studied hyperbolic geometry first. We will recall some of these models, together with their most essential properties for later use. Each model has properties which make it useful in special situations and which justify changing among models a number of times.

For the Lorentz model we list the representations for a number of hyperbolic transformations. Some of the explicit forms do not seem to be widely known. We used them especially when computing the figures of the example session.

The properties of hyperbolic circles, and the formulas we derive for the product of two rotations will be used in the proof of the comparison theorem in chapter 6.

1.1. The Lorentz Model

1.1.1. The model. The imbedding of H^n into Lorentz space $\mathbf{R}_L^{n+1}$, which is the point set $\mathbf{R}^{n+1}$ equipped with the Lorentz metric

$$\langle x, x\rangle_L := -x_0^2 + x_1^2 + ... + x_n^2 \ , \ x \in \mathbf{R}^{n+1},$$

is an imbedding into a vector space structure. It corresponds to the standard imbeddings of the other spaceforms $M^n(c)$ with constant curvature $c \in \mathbf{R}$, e.g. Euclidean and spherical geometry:

$$\begin{aligned} M^n(c) &= \left\{x \in \mathbf{R}^{n+1} \mid |x|^2 = \tfrac{1}{c}\right\}, \ c > 0 \\ M^n(0) &= \mathbf{R}^n \\ M^n(c) &= \left\{x \in \mathbf{R}_L^{n+1} \mid x_0 > 0 \ , \ |x|_L^2 = \tfrac{1}{c}\right\}, \ c < 0 \ . \end{aligned}$$

$M^n(1)$ is the n-dimensional sphere and $LM^n = M^n(-1)$ another synonym for H^n. We call the point $\mathcal{O} := (1, 0, .., 0)$ the *origin* of LM^n. Totally geodesic submanifolds of LM^n are intersections of linear subspaces of $\mathbf{R}_L^{n+1}$ with LM^n.

The *isometry group* of LM^n is generated by the rotations and reflections given by

$$\begin{pmatrix} 1 & 0 \\ 0 & O(n) \end{pmatrix},$$

which leave (1,0,..,0) fixed, and by a family of hyperbolic translations given e.g. by

$$\{T_s = \begin{pmatrix} \cosh s & \sinh s & & & & \\ \sinh s & \cosh s & & & & \\ & & 1 & & & \\ & & & . & & \\ & & & & . & \\ & & & & & 1 \end{pmatrix} \mid s \in \mathbf{R}\}.$$

The *distance* $d(x,y)$ of two points $x, y \in LM^n$ is given by

$$d(x,y) = \operatorname{arccosh}(|\langle x, y\rangle_L|).$$

Proof. . The formula is true for x =(1,0,..,0) and all points y =(cosh s, sinh s,0,..,0), $s \in \mathbf{R}$. Two arbitrary points x and y can be moved into the special position by hyperbolic isometries which do not change $\langle x,y\rangle_L$, therefore also $d(x,y)$ remains constant.

Lemma 1 [distance, angle of two geodesics]**.** *Let γ and δ be two geodesics in LM^2 with unit normal vectors N_γ and N_δ. Then the term $\left|\langle N_\gamma, N_\delta\rangle_L\right|$ determines the relative position of γ and δ:*

If $\left|\langle N_\gamma, N_\delta\rangle_L\right| \geq 1$, both geodesics have a distance

$$d(\gamma,\delta) = \operatorname{arccosh}(\left|\langle N_\gamma, N_\delta\rangle_L\right|).$$

If $\left|\langle N_\gamma, N_\delta\rangle_L\right| \leq 1$, both curves intersect at an angle

$$\alpha(\gamma,\delta) = \arccos(\left|\langle N_\gamma, N_\delta\rangle_L\right|).$$

The case $\left|\langle N_\gamma, N_\delta\rangle_L\right| = 1$ occurs when both curves have a point on S^∞ in common.

1.1.2. Geodesic connecting two points. The unit speed geodesic γ connecting two points $p, q \in LM^n$ has initial direction in p :

$$\gamma'(p) = \frac{\langle p,q\rangle_L \;\; p+q}{\sqrt{\langle p,q\rangle_L^2 - 1}}.$$

Let $y = (y_0, y_1, ..., y_n) \in LM^n$ be an arbitrary point with distance $d(\mathcal{O}, y) =$ arccosh y_0 from the origin. The unit speed geodesic γ connecting $\mathcal{O}$ and y is given by

$$\gamma(s) = \cosh s \cdot \mathcal{O} + \sinh s \cdot t \;,\; s \in [0, d(\mathcal{O}, y)]$$

$$t := \frac{1}{\sqrt{y_0^2 - 1}}(0, y_1, ..., y_n)$$

where t is the initial direction of γ.

1.1.3. Rotation around a geodesic through $\mathcal{O}$. In LM^3 a rotation around a geodesic through $\mathcal{O}$ with initial direction $t = (0, t_1, t_2, t_3)$, $|t|_L = 1$ of an angle α is given by

$$\begin{pmatrix} 1 & 0 & 0 & 0 \\ 0 & (1-\cos\alpha)t_1t_1 + \cos\alpha & (1-\cos\alpha)t_1t_2 + t_3\sin\alpha & (1-\cos\alpha)t_1t_3 - t_2\sin\alpha \\ 0 & (1-\cos\alpha)t_1t_2 - t_3\sin\alpha & (1-\cos\alpha)t_2t_2 + \cos\alpha & (1-\cos\alpha)t_2t_3 + t_1\sin\alpha \\ 0 & (1-\cos\alpha)t_1t_3 + t_2\sin\alpha & (1-\cos\alpha)t_2t_3 - t_1\sin\alpha & (1-\cos\alpha)t_3t_3 + \cos\alpha \end{pmatrix}.$$

1.1.4. Rotation around a point in infinity. Rotation around a point in infinity moves all points in LM^2 along parabolas. Let $p{=}\lim_{u\to\infty}(\cosh u, 0, \sinh u) \in S^\infty$. Then rotation around p is given by

$$Rot_{p=(\infty,0,\infty)}(s) = \begin{pmatrix} 1 + \frac{s^2}{2} & s & -\frac{s^2}{2} \\ s & 1 & -s \\ \frac{s^2}{2} & s & 1 - \frac{s^2}{2} \end{pmatrix}. \tag{1.1}$$

1.1.5. Rotation of (0,1,0,0,) to (0,t_1, t_2, t_3) in $T_{\mathcal{O}}H^3$. Let $t = (0, t_1, t_2, t_3) \neq (0, -1, 0, 0)$ then the unique rotation matrix mapping (0,1,0,0) to t around the axis (0,0,$t_3, -t_2$) in $T_{\mathcal{O}}H^3$ is given by

$$R_{\mathcal{O},(0,1,0,0)\longrightarrow t} = \begin{pmatrix} 1 & 0 & 0 & 0 \\ 0 & t_1 & -t_2 & -t_3 \\ 0 & t_2 & 1 - \frac{t_2^2}{1+t_1} & -\frac{t_2t_3}{1+t_1} \\ 0 & t_3 & -\frac{t_2t_3}{1+t_1} & 1 - \frac{t_3^2}{1+t_1} \end{pmatrix}.$$

1.1.6. Translation along the geodesic connecting $\mathcal{O}$ and a point. Let $y = (y_0, y_1, y_2, y_3)$ be an arbitrary point lying on a geodesic through $\mathcal{O}$ with initial direction $t = (0, t_1, t_2, t_3) \neq (0, -1, 0, 0)$ in $\mathcal{O}$. Then the translation along the geodesic γ connecting $\mathcal{O}$ and y is given by

$$T_{\mathcal{O}\longrightarrow\gamma(s)} = R_{\mathcal{O},(0,1,0,0)\longrightarrow t} \circ T_s \circ {}^tR_{\mathcal{O},(0,1,0,0)\longrightarrow t}$$

$$= \begin{pmatrix} \cosh s & t_1\sinh s & t_2\sinh s & t_3\sinh s \\ t_1\sinh s & t_1^2(\cosh s - 1) + 1 & t_1t_2(\cosh s - 1) & t_1t_3(\cosh s - 1) \\ t_2\sinh s & t_1t_2(\cosh s - 1) & t_2^2(\cosh s - 1) + 1 & t_2t_3(\cosh s - 1) \\ t_3\sinh s & t_1t_3(\cosh s - 1) & t_2t_3(\cosh s - 1) & t_3^2(\cosh s - 1) + 1 \end{pmatrix}.$$

1.1.7. Totally geodesic hyperplanes and normal vectors. Every vector $N \in \mathbf{R}_L^{n+1}$ with $\langle N, N\rangle_L = 1$ determines uniquely a totally geodesic hyperplane H_N via

$$H_N = \{p \in LM^n \mid \langle N, p\rangle_L = 0\}.$$

The map $\{N, -N\} \to H_N$ is a bijection between the set of all normal vector pairs and all hyperplanes. The vector N of a hyperplane H_N is independent of the base point and therefore well-defined.

Given three points $P, Q, R \in LM^3$ not lying on a single geodesic. The normal vector N of the hyperplane spanned by P, Q, R is determined as the solution of $\langle P, N\rangle_L = \langle Q, N\rangle_L = \langle R, N\rangle_L = 0$, $\langle N, N\rangle_L = 1$. Writing $P = (p_0, p_1, p_2, p_3)$, $Q = (q_0, q_1, q_2, q_3)$, $R = (r_0, r_1, r_2, r_3)$ this leads to a linear system of equations

$$\begin{vmatrix} p_0 & q_0 & r_0 & -u_0 \\ p_1 & q_1 & r_1 & u_1 \\ p_2 & q_2 & r_2 & u_2 \\ p_3 & q_3 & r_3 & u_3 \end{vmatrix} = 0$$

which is solved by

$$u_0 = \begin{vmatrix} p_1 & q_1 & r_1 \\ p_2 & q_2 & r_2 \\ p_3 & q_3 & r_3 \end{vmatrix}, \; u_1 = \begin{vmatrix} p_0 & q_0 & r_0 \\ p_2 & q_2 & r_2 \\ p_3 & q_3 & r_3 \end{vmatrix}, \; u_2 = -\begin{vmatrix} p_0 & q_0 & r_0 \\ p_1 & q_1 & r_1 \\ p_3 & q_3 & r_3 \end{vmatrix}, \; u_3 = \begin{vmatrix} p_0 & q_0 & r_0 \\ p_1 & q_1 & r_1 \\ p_2 & q_2 & r_2 \end{vmatrix}.$$

After normalizing the solution vector we obtain the normal vector N by

$$N = (u_0, u_1, u_2, u_3) \cdot \frac{1}{\sqrt{-u_0^2 + u_1^2 + u_2^2 + u_3^2}}.$$

The minus sign of u_0 in the matrix of the equation reflects the Lorentzian scalar product.

1.1.8. Reflection at a hyperplane. Let $N = (u_0, u_1, u_2, u_3)$ be the normal vector of an arbitrary hyperplane $H_N \subset LM^3$. Then the hyperbolic reflection at the hyperplane H_N is defined by

$$P \xrightarrow{reflection} P - 2\langle P, N\rangle_L \cdot N, \; P \in LM^3.$$

This is a linear map $S_N = id - 2\langle \, . \, , N\rangle_L \cdot N$ whose matrix S_N is given by

$$\begin{pmatrix} 1+2u_0^2 & -2u_0u_1 & -2u_0u_2 & -2u_0u_3 \\ 2u_0u_1 & 1-2u_1^2 & -2u_1u_2 & -2u_1u_3 \\ 2u_0u_2 & -2u_1u_2 & 1-2u_2^2 & -2u_2u_3 \\ 2u_0u_3 & -2u_1u_3 & -2u_2u_3 & 1-2u_3^2 \end{pmatrix}.$$

1.2. The Poincaré Ball Model

The Poincaré model PM^n of hyperbolic space H^n is the interior of the n-dimensional unit ball in $\mathbf{R}^{n+1}$. The asymptotic boundary is denoted by S^∞. The metric given by

$$ds^2 = \frac{4}{\left(1-|z|^2\right)^2}\, dx^2$$

is conformal to the Euclidean metric. Totally geodesic submanifolds are intersections of those Euclidean spheres with PM^n which intersect S^∞ orthogonally.

Let $z, w \in PM^2$ be two complex numbers. Then the distance function d is given by

$$d(z,w) = \log \frac{|1-z\overline{w}| + |z-w|}{|1-z\overline{w}| - |z-w|}$$

and the isometry group is given by

$$\left\{ z \mapsto \frac{az+\overline{c}}{cz+\overline{a}} \right\} \cup \left\{ z \mapsto \frac{a\overline{z}+\overline{c}}{c\overline{z}+\overline{a}} \right\} \text{ where } |a|^2 - |c|^2 = 1,\ \text{a,c} \in \mathbf{C}.$$

The isometries of PM^3 extend naturally to S^∞. Identifying S^∞ with $\widehat{\mathbf{C}}$ via stereographic projection, the hyperbolic isometry group is isomorphic to the automorphism group of $\widehat{\mathbf{C}}$.

The Poincaré model may be obtained from Lorentz model LM^n by central projection of LM^n with center (-1,0,..,0) onto the interior of the unit ball in the hyperplane $\{x_0 \equiv 0\}$. This projection is conformal.

1.3. The Klein Ball Model

Using a different projection we obtain the Klein model KM^n. It also sits inside the n-dimensional unit ball in $\mathbf{R}^{n+1}$ but the metric is not conformal to the Euclidean. Using (0,..,0) in $\mathbf{R}^{n+1}_L$ as a center the Klein model is obtained by projecting LM^n into the interior of the unit ball of the hyperplane $\{x_0 \equiv 1\}$ in $\mathbf{R}^{n+1}_L$. Totally geodesic submanifolds are intersections of Euclidean planes $\mathbf{R}^{n+1}_L$ with $\{x_0 = 1\}$.

Let $p, q \in KM^n$ be two points inside the unit ball. Then their hyperbolic distance is given by

$$d(p,q) = \operatorname{arccosh}\left(\frac{1-\langle p,q\rangle}{\sqrt{(1-|p|)\cdot(1-|q|)}} \right),$$

where the Euclidean metric is used on the right side.

1.4. The Upper Halfspace Model

1.4.1. The model. A further model of H^n is the upper halfspace model UHM^n. It consists of the open upper halfspace $\{x_n > 0\}$ in $\mathbf{R}^n$ with the metric

$$ds^2 = \frac{1}{x_n^2}\, dx^2.$$

The hyperplane $\{x_n \equiv 0\} \cup \infty$ is the sphere at infinity S^∞. Totally geodesic submanifolds are all half spheres and half planes intersecting S^∞ orthogonally. Hyperplanes parallel to $\{x_n \equiv 0\}$ are horospheres with constant curvature 1. Euclidean planes are hyperbolic spheres with constant curvature $\kappa \in [0,1]$ depending on the angle under which they intersect S^∞. See lemma 3.

In dimension 2 the UHM is part of the complex plane and the distance function between two points is given by

$$d(z,w) = \log \frac{|z-\overline{w}| + |z-w|}{|z-\overline{w}| - |z-w|}.$$

The isometry group is given by

$$\left\{ z \mapsto \frac{az+b}{cz+d} \right\} \cup \left\{ z \mapsto \frac{-a\overline{z}+b}{-c\overline{z}+d} \right\},\ ad-bc>0,\ \text{where } a,b,c,d \in \mathbf{R}.$$

1.4.2. A translation in the LM, PM and UHM. A translational isometry

$$p \in LM^n \mapsto \begin{pmatrix} \cosh r & & & & \sinh r \\ & 1 & & & \\ & & \cdot & & \\ & & & \cdot & \\ & & & & 1 \\ \sinh r & & & & \cosh r \end{pmatrix} \cdot p$$

in LM^n along the geodesic $(\cosh r, 0, .., 0, \sinh r)$ translates in PM^n along the geodesic through (0,..,0) in direction x_n and in UHM^n along the geodesic through (0,..,0) in direction x_n by

$$p \in UHM^n \mapsto \frac{1}{\cosh r - \sinh r}\ p = \mathrm{e}^r \cdot p\ .$$

So the orbits of this translation are Euclidean straight lines with center (0,..,0). Intrinsicly these lines are circles with curvature $\kappa \in [0,1)$. In UHM^2 those circles with $\kappa \in (0,1)$ may be parametrized by arc length s via

$$\gamma_\kappa(s) = e^{s \cdot \sin\alpha} \cdot \begin{pmatrix} \cos\alpha \\ \sin\alpha \end{pmatrix},\ s \in \mathbf{R}$$

where $\kappa = \cos\alpha$ and α is the Euclidean and hyperbolic angle under which γ intersects S^∞.

1.5. Projection Between Standard Models

During the numerical computations we used the following maps and their differentials between the different models. We list them as a reference.

1.5.1. Lorentz model and Poincaré ball. Central projection with center (-1,0,..,0) into unit ball in $\{x_0 \equiv 0\}$:

$$LM^n \longrightarrow PM^n \qquad (x_0, ..., x_n) \mapsto \left(0, \tfrac{x_1}{1+x_0}, ..., \tfrac{x_n}{1+x_0}\right)$$

$$PM^n \longrightarrow LM^n \qquad y := (y_1, ..., y_n) \mapsto (t, (1+t)y_1, ..., (1+t)y_n)$$

$$\text{with} \quad t := \tfrac{1+|y|^2}{1-|y|^2} \ , \quad t+1 = \tfrac{2}{1-|y|^2} \ , \quad t_{y_i} := \tfrac{\partial}{\partial y_i} t = y_i(1+t)^2$$

$$\text{and differential} \quad \begin{pmatrix} t_{y_1} & t_{y_2} & \cdot & \cdot & t_{y_n} \\ t_{y_1} \cdot y_1 + 1 + t & t_{y_2} \cdot y_1 & \cdot & \cdot & t_{y_n} \cdot y_1 \\ \cdot & \cdot & & & \cdot \\ \cdot & \cdot & & & \cdot \\ t_{y_1} \cdot y_n & t_{y_2} \cdot y_n & \cdot & \cdot & t_{y_n} \cdot y_n + 1 + t \end{pmatrix}.$$

1.5.2. Lorentz model and Klein ball. Central projection with center (0,..,0) into the unit ball in $\{x_0 \equiv 1\}$ gives a map from LM^n into KM^n :

$$LM^n \to KM^n \qquad (x_0, ..., x_n) \mapsto \left(1, \tfrac{x_1}{x_0}, ..., \tfrac{x_n}{x_0}\right)$$

$$KM^n \longrightarrow LM^n \qquad y := (y_1, ..., y_n) \mapsto (t, ty_1, ..., ty_n)$$

$$\text{with} \quad t = (1 - |y|^2)^{-\frac{1}{2}}, \quad t_{y_i} := \tfrac{\partial}{\partial y_i} t = y_i \cdot t^3$$

$$\text{and differential} \quad \begin{pmatrix} t_{y_1} & t_{y_2} & \cdot & \cdot & t_{y_n} \\ t_{y_1} \cdot y_1 + t & t_{y_2} \cdot y_1 & \cdot & \cdot & t_{y_n} \cdot y_1 \\ \cdot & \cdot & & & \cdot \\ \cdot & \cdot & & & \cdot \\ t_{y_1} \cdot y_n & t_{y_2} \cdot y_n & \cdot & \cdot & t_{y_n} \cdot y_n + t \end{pmatrix}.$$

1.5.3. Poincaré ball and upper halfspace. A Möbius transformation may be used to transform the Poincaré ball PM^2 in UHM^2 :

$$PM^2 \longrightarrow UHM^2 \qquad z \mapsto -i \cdot \tfrac{z+i}{z-i} \ ,$$

$$\text{where} \quad i \mapsto \infty, \quad 0 \mapsto i, \quad -i \mapsto 0, \quad \pm 1 \mapsto \pm 1,$$

and in general by

$$PM^n \longrightarrow UHM^n \qquad (x_1, ..., x_n) \mapsto \tfrac{(2x_1, ..., 2x_{n-1}, 1-|x|^2)}{x_1^2 + ... + x_{n-1}^2 + (x_n - 1)^2} \ .$$

The inverse mapping is given by

$$UHM^n \longrightarrow PM^n \qquad (y_1, ..., y_n) \mapsto \tfrac{(2y_1, ..., 2y_{n-1}, |y|^2 - 1)}{y_1^2 + ... + y_{n-1}^2 + (y_n + 1)^2} \ .$$

1.5.4. Klein ball and upper halfspace model. The previous transformations may be composed to get a map from Klein ball KM^n into UHM^n :

$$\begin{array}{ll} KM^n \longrightarrow UHM^n & (x_1,...,x_n) \mapsto \frac{(x_1,...,x_{n-1},1-\frac{|x|^2}{1+\sqrt{1-|x|^2}})}{1-x_n} \\ UHM^n \longrightarrow KM^n & (y_1,...,y_n) \mapsto \frac{(2y_1,...,2y_{n-1},|y|^2-1)}{1+|y|^2}. \end{array}$$

1.5.5. Lorentz model and upper halfspace model. This transformation is of a very simple form:

$$\begin{array}{ll} LM^n \longrightarrow UHM^n & (x_0,...,x_n) \mapsto \frac{(x_1,...,x_{n-1},1)}{x_0-x_n} \\ UHM^n \longrightarrow LM^n & (y_1,...,y_n) \mapsto \frac{(1+|y|^2,2y_1,...,2y_{n-1},|y|^2-1)}{2y_n}. \end{array}$$

1.5.6. Poincaré ball and Klein ball. A transformation between both ball models is given by the following maps:

$$\begin{array}{ll} PM^n \longrightarrow KM^n & (x_1,...,x_n) \mapsto \frac{2}{1-|x|^2}(x_1,...,x_n) \\ KM^n \longrightarrow PM^n & (y_1,...,y_n) \mapsto \frac{1}{1+\sqrt{1-|y|^2}}(y_1,...,y_n). \end{array}$$

1.6. Hyperbolic Trigonometry

Without proof we list the following frequently used hyperbolic trigonometric formulas. For a detailed study of hyperbolic trigonometry we refer to the nice book of Beardon [3].

Let Δ be a hyperbolic triangle in $LM^n \subset \mathbf{R}^{n+1}_L$ with vertices $A, B, C \in LM^n$, side lengths a, b, c and angles α, β, γ as indicated in figure 1.1.

The following relations hold:

$$\begin{aligned} \operatorname{area}(\Delta) &= \pi - \alpha - \beta - \gamma \\ \cosh c &= -\langle A, B\rangle_L \\ \cos\gamma &= \frac{\langle A,C\rangle_L \langle B,C\rangle_L + \langle A,B\rangle_L}{\sqrt{1-\langle A,C\rangle_L^2}\sqrt{1-\langle B,C\rangle_L^2}} \end{aligned}$$

Sine Rule:

$$\frac{\sinh a}{\sin\alpha} = \frac{\sinh b}{\sin\beta} = \frac{\sinh c}{\sin\gamma} \tag{1.2}$$

Cosine Rule I:

$$\cosh c = \cosh a \cosh b - \sinh a \sinh b \cos\gamma \tag{1.3}$$

Cosine Rule II:

$$\cosh c = \frac{\cos\alpha\cos\beta + \cos\gamma}{\sin\alpha\sin\beta} \tag{1.4}$$

1.7. Circles in Hyperbolic Space

In the comparison theorems for planar curves in chapter 6 we compare planar curves with arcs of hyperbolic circles. Here we discuss circles as orbits of hyperbolic isometries and derive some other useful properties for later use.

Circles in hyperbolic space are planar curves with constant curvature. As an effect of the intrinsic negative curvature of H^n, there exist three types of circles in H^2 and three types of hyperspheres in higher dimensions depending on their curvature κ. E.g. in LM^2 circles are represented by Euclidean circles, parabolas and hyperbolas on $LM^2 \subset \mathbf{R}^3_L$.

1.) Let $\kappa \in (1, \infty)$ and γ_κ a circle with curvature κ. Then γ_κ is a Euclidean circle in all models of H^2 we have discussed. In LM^2 γ_κ may be given as the orbit of a rotation with center $\mathcal{O}$. Parameterized by arc length s, we obtain

$$\gamma_\kappa(s) = \begin{pmatrix} 1 & & \\ & \cos\frac{s}{\sinh r} & -\sin\frac{s}{\sinh r} \\ & \sin\frac{s}{\sinh r} & \cos\frac{s}{\sinh r} \end{pmatrix} \begin{pmatrix} \cosh r \\ \sinh r \\ 0 \end{pmatrix}, \; s \in [0, l]$$

$$\begin{array}{llcl} \text{with} & \text{radius} & r & = & \operatorname{arccoth}\kappa \\ & \text{perimeter} & l & = & 2\pi \sinh r \\ & \text{area} & \Omega & = & 2\pi(\cosh r - 1) = 4\pi \cdot \sinh^2 \frac{r}{2}. \end{array}$$

If the curvature κ decreases to 1, the radius becomes infinitely large. In the limit, $\kappa = 1$, we obtain a horocircle (or horosphere in higher dimensions) whose center lies on S^∞.

For additional formulas concerning a sector of a hyperbolic circle compare lemma 31 in chapter 6.

2.) An arc length parameterization of horocircles with $\kappa = 1$ may be easily obtained by using the UHM^n. Euclidean straight lines parallel to $x_n \equiv 0$ are horocircles with center in ∞. Let

$$\widetilde{\gamma}(s, r) = \begin{pmatrix} rs \\ r \end{pmatrix}$$

denote such a curve in UHM^2 with arc length parameter s and at a constant height $r = x_2$. These curves project into LM^2 to a horocircle

$$\gamma_1(s, r) = \begin{pmatrix} \frac{r^2(s^2+1)+1}{2r} \\ s \\ \frac{r^2(s^2+1)-1}{2r} \end{pmatrix}, \; s \text{ arc length.}$$

Substituting

$$r = \cosh x \; + \; \sinh x = e^x \; , \; \frac{1}{r} = \cosh x \; - \; \sinh x$$

such that

$$\frac{1+r^2}{2r} \to \cosh x \ , \ \frac{-1+r^2}{2r} \to \sinh x$$

we obtain an arc length representation of a family of horocircles in LM^2 around the point on S^∞, which is the limit of $(\cosh x, 0, \sinh x)$ for $x \longrightarrow \infty$:

$$\gamma_1(s,x) = \begin{pmatrix} \frac{s^2}{2} \cdot e^{-x} + \cosh x \\ s \\ \frac{s^2}{2} \cdot e^{-x} + \sinh x \end{pmatrix}.$$

x is the distance of the circle $\gamma_1(.,x)$ to the origin $\mathcal{O} = (1,0,0,0)$. Rotation around a point on S^∞ is described by the map 1.1. This circle is not closed but both ends have the same limit on S^∞. In the PM such a circle is a Euclidean circle tangent to its hyperbolic center on S^∞.

3.) Rotating around a point p beyond infinity leads to circles with curvature $\kappa \in [0,1)$. Consider PM^2 or KM^2 and the two Euclidean lines through p and tangent to S^∞. Segments of Euclidean circles through the two points of tangency on S^∞ are hyperbolic circles with curvature $\kappa \in [0,1)$. They do not close in H^2. The circles are orbits of the unique geodesic δ connecting the two points of tangency. Assume δ is given by $\delta(s) = (\cosh s, \sinh s, 0)$, the translation along δ by

$$T(s) = \begin{pmatrix} \cosh s & \sinh s & 0 \\ \sinh s & \cosh s & 0 \\ 0 & 0 & 1 \end{pmatrix}$$

and let

$$q = \begin{pmatrix} \cosh r \\ 0 \\ \sinh r \end{pmatrix} \in H^2$$

be a point of distance r to δ. Then the orbit γ_κ of q is a circle of curvature $\kappa \in [0,1)$ given by

$$\gamma_\kappa(s) = \begin{pmatrix} \cosh s & \sinh s & 0 \\ \sinh s & \cosh s & 0 \\ 0 & 0 & 1 \end{pmatrix} \begin{pmatrix} \cosh r \\ 0 \\ \sinh r \end{pmatrix}$$

with distance $r = \operatorname{arctanh} \kappa$ of δ to γ_κ.

The following lemma derives the cone angle under which a hyperplane appears in a hyperbolic view (see figure 1.2). The formula gives the opening angle of the cone enclosed by the geodesics through a point and the asymptotic boundary of a hyperplane in H^n.

Lemma 2 [cone angle]**.** *Let γ be a geodesic with endpoints $q_1, q_2 \in S^\infty$ and $p \notin \gamma$ a point in H^2. Then the geodesics δ_1, δ_2 connecting p with q_1, q_2 form a cone with angle ψ given by*

$$\cot\frac{\psi}{2} = \sinh r$$

where $r = dist(p, \gamma)$. Furthermore for a given geodesic γ all points with the same cone angle ψ lie on a circle through q_1, q_2 with curvature $\kappa = \tanh r$ and distance r to γ.

Proof. . The geodesics $\gamma, \delta_1, \delta_2$ form a hyperbolic triangle with two ideal points, i.e. two triangle angles vanish. Using Cosine Rule II we obtain the proposed formula.

The second statement follows immediately from the invariance of the formula under the position of the circle γ_κ with $\kappa = \tanh r$.

We now derive the angle between a hyperbolic geodesic and a circle joining the same two points on S^∞ (compare figure 1.2).

Lemma 3 [angle at ∞]**.** *Let γ be a geodesic and γ_κ a circle with curvature $\kappa \in [0, 1)$. If both curves have the same two points on S^∞ as asymptotic boundary, then the asymptotic angle φ between both curves is given by*

$$\tan\varphi = \sinh r$$

where $r := dist\,(\delta, \gamma_\kappa) = \operatorname{arctanh}\kappa$.

Furthermore each geodesic δ_1 or δ_2 through one of the asymptotic boundary points and intersecting γ_κ somewhere else in a point p encloses the same angle φ at the intersection point p with γ_κ.

Proof. . The angle φ at p between δ_1, δ_2 and γ_κ can be obtained using the result of lemma 2 on the cone angle ψ between δ_1 and δ_2. γ is parallel to δ_1, δ_2 at S^∞, and δ_1, δ_2 and γ_κ are circles in the conformal Poincaré model. Therefore the angle between γ and γ_κ at q_1, q_2 is the same φ as between δ_1, δ_2 and γ_κ in p.

1.8. Product of Two Rotations

In this section we consider the effect of a product of two rotations in the hyperbolic plane and derive formulas for the occurring angles. We use these results in the proof of the comparison theorem for planar curves in chapter 6. Let

$$g = rot_p(\theta)$$
$$h = rot_q(\phi)$$

be two rotations around disjoint center points $p, q \in H^2$ and angles θ and ϕ. As in the Euclidean case the product $h \circ g$ results in either a rotation around a center s or in a translation. We write g and h as a product of two reflections

$$g = \sigma_2 \circ \sigma_1$$
$$h = \sigma_4 \circ \sigma_3$$

where the lines of reflection σ_1 and σ_2 resp. σ_3 and σ_4 enclose angles $\frac{\theta}{2}$ resp. $\frac{\phi}{2}$. We choose the two lines of reflection σ_2 and σ_3 to be the unique geodesic σ connecting p and q. Then the product $h \circ g$ is given by:

$$h \circ g = \sigma_4 \circ \sigma_1.$$

Lemma 4. *The product of two rotations g and h results in one of the two following cases:*

- *if σ_1 and σ_4 intersect in $s \in H^2 \cup S^\infty$, then $h \circ g$ is a rotation around s*
- *if σ_1 and σ_4 do not intersect, then $h \circ g$ is a translation along the shortest geodesic T connecting σ_1 and σ_4.*

In the special case of two rotations g and h around center points p and q with angles θ and -θ the product $h \circ g$ is a translation along the shortest geodesic T connecting σ_1 and σ_4. T is orthogonal to σ_1 and σ_4 and it encloses with σ_1 and σ resp. σ_4 and σ two conformal, and therefore congruent triangles. From this and from the use of the sine rule and cosine rules 1.2, 1.4, we have the following equations for the distance of translation $d = 2 \cdot dist(\sigma_1, \sigma_4)$ and the angle $\frac{\pi}{2} - \tilde{\theta}$ enclosed by T and σ (compare figure 1.3):

$$\tan \tilde{\theta} = \cot\left(\frac{\pi}{2} - \tilde{\theta}\right) = \cosh \frac{dist(p,q)}{2} \cdot \tan \frac{\theta}{2} \tag{1.5}$$

$$\sinh \frac{d}{4} = \sinh \frac{dist(p,q)}{2} \cdot \sin \frac{\theta}{2} \tag{1.6}$$

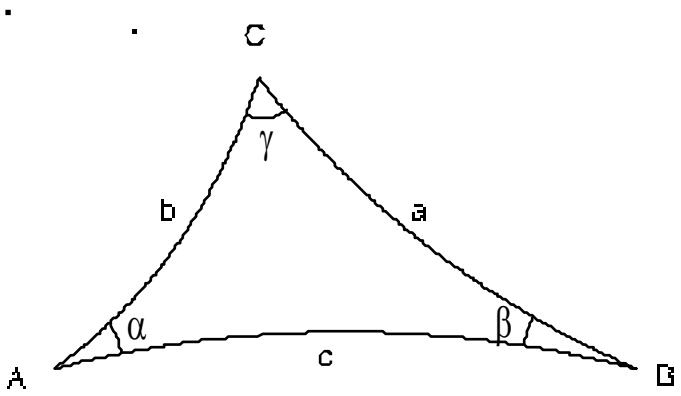

Figure 1.1: Notation in a Hyperbolic Triangle

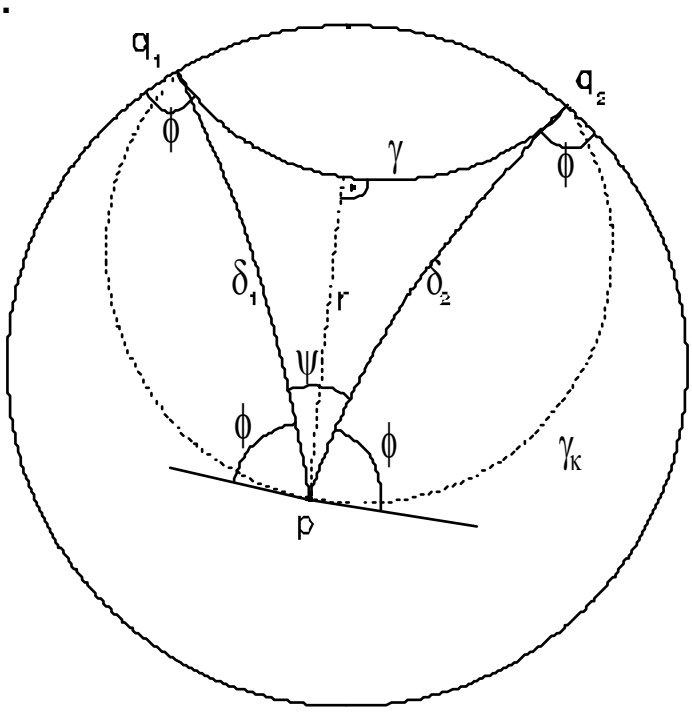

Figure 1.2: Cone Angle Under Which a Hypersurface Appears From a Point

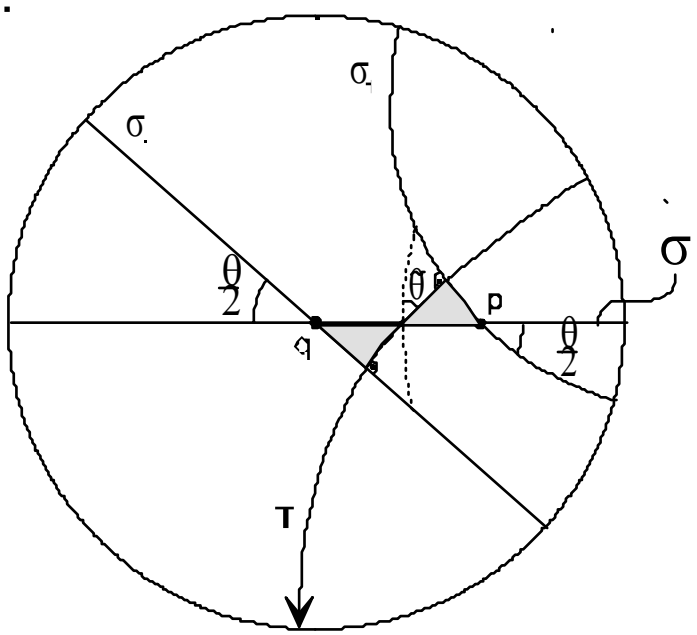

Figure 1.3: Product of Two Rotations

Chapter 2

Properties of Hyperbolic Minimal Surfaces

In this chapter we recall well-known results for hyperbolic minimal surfaces. We give the notion of minimal surfaces in parametric and non-parametric form since we will use both. When deriving the geometric a prior estimates in chapter 4 we use the parametric form, while the proof of the existence theorem 29 is based on the minimal surface equation 2.1 in the non-parametric form.

2.1. The Hyperbolic Minimal Surface Equation

We call a surface $M \subset H^3$ in the upper halfspace model a graph if M projects 1-1 along the vertical lines on a domain $\Omega \subset \mathbf{C}$. Then M can be represented by a function

$$f : \Omega \to \mathbf{R}.$$

The hyperbolic area of M over compact subsets $K \subset \Omega$ is given by

$$area(f_{|K}) = \int_K \frac{\sqrt{1 + |df|^2}}{f^2} dz.$$

The hyperbolic minimal surface equation for M resp. f is the Euler-Lagrange equation of the above variational integral, where (x, y) are local coordinates in Ω:

$$(1 + f_y^2) f_{xx} - 2 f_x f_y f_{xy} + (1 + f_x^2) f_{yy} + \frac{2(1 + f_x^2 + f_y^2)}{f} = 0 \text{ in } \Omega. \tag{2.1}$$

The equation consists of the terms of the Euclidean minimal surface equation and an additional quotient. It is a quasilinear, non-uniformly elliptic equation with singular behavior when f tends to zero. This is the case at the asymptotic boundary of M.

In chapter 5 we will study this differential equation in greater detail. There we consider boundary data

$$\varphi : \partial\Omega \to \mathbf{R}_0^+$$

on $\partial\Omega$ which is positive but may also be zero, i.e. we need to get control of the singular behavior of the equation. This will be possible since the geometry of the solutions can be controlled.

Additional properties immediately follow from the hyperbolic geometry. Half-spheres with center $p \in \mathbf{C}$ and radius r given by

$$f_{p,r}(z) = \sqrt{r^2 - (z-p)^2}$$

are trivial solutions. Also the scaling invariance w.r.t. a point $p \in \mathbf{C}$ is an immediate consequence of the effect of a hyperbolic translation along the vertical geodesic through p, whose orbits are straight lines through p. See section 1.4.2. Therefore, if f is a solution of 2.1 then also f_r defined by

$$f_r(z) := \frac{f(rz)}{r},\ \Omega_r = \{z \in \mathbf{C} \mid rz \in \Omega\},$$

where we have chosen $p = 0 \in \mathbf{C}$. Since the translation is an isometry we have further

$$area(f_{r|\Omega_r}) = area(f_{|\Omega}).$$

2.2. Associated Family

Let M^2 be a simply connected piece of a Riemann surface. Then the map

$$F : M^2 \longrightarrow H^3$$

is a **minimal immersion** iff the mean curvature H of $F(M^2)$ vanishes identically.

Let F denote a minimal immersion in the following. We denote with g the induced metric on M and with S the Weingarten map defined by $g(Su, v) := < \partial F \cdot u, \partial N \cdot v >$ for tangent vectors u and v of M and normal vector N of $F(M)$.

Then for each such F there exists an isometric family

$$F^\theta : M^2 \longrightarrow H^3,\ \theta \in [0, 2\pi]$$

of minimal surfaces with geometric data

$$\begin{aligned} g^\theta &= g \\ S^\theta &= D^\theta \cdot S, \end{aligned}$$

where D^θ denotes the rotation about θ of the oriented tangent plane in M^2. Since F is minimal, the tensor S^θ is also symmetric with trace $S^\theta = 0$. The family F^θ is called the **associated family** of F, and the map $F^{\frac{\pi}{2}}$ is called the **conjugate immersion** of F.

Minimal surfaces in simply connected three dimensional spaceforms have a nice symmetry property in common. If a minimal surface has a boundary arc which is part of a geodesic of the ambient spaceform then the surface may be extended to a larger minimal surface by rotating a copy about 180° around the geodesic. If the surface contains a boundary arc which is a geodesic of the surface and lies in a hyperplane of the spaceform, then the surface may be extended by reflection at the hyperplane.

Both methods extend the original surface analytically across the boundary arc. These properties were originally discovered by H.A. Schwarz for minimal surfaces in $\mathbf{R}^3$ and later extended by Lawson [19] to minimal surfaces in spaceforms.

In this notation the Frenet data of a geodesic $F^\theta \cdot c$ with the frame $(\partial F^\theta \cdot \dot{c}, N, \partial F^\theta \cdot D^{\frac{\pi}{2}}\dot{c})$ on a minimal surface is given by

$$\begin{array}{rcccccc} curvature(c) & = & \kappa^\theta & = & g(S^\theta \dot{c}, \dot{c}) & = & -\tau^{\theta+\frac{\pi}{2}} \\ torsion(c) & = & \tau^\theta & = & g(S^\theta \dot{c}, D^{\frac{\pi}{2}}\dot{c}) & = & \kappa^{\theta+\frac{\pi}{2}}. \end{array}$$

Therefore a straight line is a planar geodesic on the conjugate immersion and vice versa a planar geodesic becomes a straight line.

2.3. Maximum Principle

The maximum principle for surfaces of constant mean curvature in spaceforms is a powerful tool and we will apply it frequently through our constructions.

Definition 5. *Let M and N be two hypersurfaces in H^3 with first order of contact at an interior point p, i.e. $p \in \overset{\circ}{M} \cap \overset{\circ}{N}$ and the tangent planes in p correspond $T_pM = T_pN$. Then we say M* lies on one side *of $N :\Leftrightarrow$ when writing M and N locally as a graph over the tangent plane with function f_M and f_N then $f_M \geq f_N$ or $f_M \leq f_N$ in a neighbourhood of p.*

There exist a number of different proofs for the following maximum principle. We cite Eschenburg [7], who uses mostly geometric arguments in his proof:

Lemma 6 [Maximum Principle]**.** *Let M and N be two smooth hypersurfaces in H^3 with the same constant mean curvature and common point p in the interior or on the boundary of M resp. N. If M lies on one side of N in a small neighbourhood of p, then M and N are identical close to p, and therefore analytic continuations of each other.*

2.4. A System of Differential Equations

Let $F : \Omega \subset \mathbf{R}^2 \longrightarrow LM^3 \subset \mathbf{R}^4_L$ be a conformal parametrisation of a hyperbolic minimal surface. Using local coordinates (u, v) on Ω we denote the induced metric on Ω with

$$ds^2 = E(du^2 + dv^2)$$

and the second fundamental form with

$$II = e(du^2 - dv^2) + 2f dudv.$$

Then F satisfies the following system of equations

$$\begin{pmatrix} F_{uu} \\ F_{uv} \\ F_{vv} \\ N_u \\ N_v \end{pmatrix} = \begin{pmatrix} E & \frac{E_u}{2E} & \frac{-E_v}{2E} & -e \\ 0 & \frac{E_v}{2E} & \frac{E_u}{2E} & -f \\ E & \frac{-E_u}{2E} & \frac{E_v}{2E} & e \\ 0 & \frac{e}{E} & \frac{f}{E} & 0 \\ 0 & \frac{f}{E} & \frac{-e}{E} & 0 \end{pmatrix} \cdot \begin{pmatrix} F \\ F_u \\ F_v \\ N \end{pmatrix} \tag{2.2}$$

where F, its partial derivatives and N are given as vectors in $\mathbf{R}^4_L$ and the triple (F_u, F_v, N) is positive oriented.

Using the system of equations and the Mainardi-Codazzi equations $e_u + f_v = e_v - f_u = 0$ we immediately obtain two elliptic equations

$$\begin{aligned} \triangle F &= 2F \\ \triangle N &= -|A|^2 N \end{aligned}$$

where $\triangle = \frac{1}{E}(\partial_{uu} + \partial_{vv})$ is the laplacian on Ω w.r.t. the induced metric and $|A|^2 = \frac{e^2+f^2}{E^2}$ the norm of the second fundamental form.

2.5. Convexity and Convex Hull

We note some useful properties of minimal surfaces in H^3 concerning their convex hull. The main ingredient in the proofs is the maximum principle.

The definition of p-convexity for curves on the asymptotic sphere will be used in the specification of admissible contours $\Gamma \subset H^3 \cup S^\infty$ for the existence theorem 29.

Definition 7. *A* **halfspace** *H of hyperbolic space is defined as one of the components in which a totally geodesic plane P divides $H^3 \cup S^\infty$. The halfspace includes the plane P and its asymptotic limit.*

The **convex hull** *$C(S)$ of a subset $S \subset H^3 \cup S^\infty$ is defined as the intersection of all closed halfspaces H containing S.*

Lemma 8 [Convex Hull Principle]**.** *Let $\Gamma \subset H^3 \cup S^\infty$ be the boundary of a regular minimal surface M in H^3. Then*

$$M \subset C(\Gamma).$$

Proof. . Let P be a hyperbolic plane dividing H^3 into two open halfspaces H^+ and H^- such that $C(\Gamma) \subset H^- \cup P$. We show by contradiction that M must also lie in $H^- \cup P$.

Assume $M \cap H^+ \neq \emptyset$. Then there exists a point q on $M \cap H^+$ having maximal finite distance from P. The tangent plane T_qM locally bounds M to one of its sides and is therefore a contradiction to the maximum principle.

Lemma 9. *Let $\Gamma \subset S^\infty$ be a curve and the boundary of a regular minimal surface M in H^3. Then*

$$\Gamma = S^\infty \cap C(M).$$

Proof. . For each point $q \in S^\infty \backslash \Gamma$ we can find a hyperbolic plane separating $H^3 \cup S^\infty$ into two components such that q and M lie in different halfspaces. In the Poincaré model a small Euclidean sphere around q would give such a hyperbolic plane. Therefore $q \notin C(M)$.

We need the term "convex" for subsets on hyperbolic spheres and on S^∞. This term is well-defined for spheres by their intrinsic geometry, but for a useful definition on S^∞ we need to specialize.

Definition 10. *A compact closed curve Γ on a sphere $S \subset H^3$ of constant curvature $\kappa \geq 0$ is* **convex** *:⇔ every totally geodesic plane intersecting S orthogonally and of tangency to Γ restricts Γ to one of the halfspaces defined by the plane.*

This definition agrees with the intrinsic term convex of the sphere. We extend it to curves on S^∞ in the following way:

Definition 11 [p-Convexity]**.** *Let $p \in S^\infty$ be a point in the asymptotic boundary of H^3. A compact closed curve $\Gamma \subset S^\infty$ is* **p-convex** *:⇔ every totally geodesic plane containing p, whose asymptotic boundary is tangent to Γ, restricts Γ to one of the halfspaces defined by the plane.*

When projecting H^3 into the UHM with $p \to \infty$, a p-convex curve $\Gamma \subset S^\infty$ not containing p projects onto a curve in $\mathbf{C}$ which is convex w.r.t. the Euclidean metric of $\mathbf{C}$. Vice versa, each convex curve in $\mathbf{C}$ in this UHM is p-convex, but in general not convex w.r.t. the spherical geometry.

Our definition of p-convexity uses the intrinsic geometry of hyperbolic space instead of the Euclidean metric on $\mathbf{C}$. Later we will need the property "p-convexity" w.r.t. different points $p \in S^\infty$, therefore a definition not depending on a specific UHM is advantageous.

Chapter 3

C^0-Estimates for Minimal Graphs

The C^0-estimates we use in our work base on a comparison of a contour or a minimal surface with a well-known minimal surface and the application of the maximum principle. In section 2.5 we discussed the convex hull property as the simplest C^0-estimate. In the following we make this property explicit for minimal surfaces given as a graph in the UHM and obtain C^0 bounds for the solution of the minimal surface equation 2.1.

In theorem 24 we use the translated copy of a given minimal surface as a barrier. Other useful barrier surfaces are the hyperbolic catenoids and the helicoids, since they are embedded, explicitly given and occur as a 1-parameter family. The conjugate surface construction for minimal surfaces in chapter 8 relies on our ability of estimating the turning angle of the surface normal against a parallel vector field along a straight boundary arc. For this estimate we use hyperbolic helicoids having the straight arc as their soal and keeping the minimal surface to one of its sides. We discuss this in more detail in the chapters 6 and 8.

In case of minimal graphs in the upper halfspace model we can specialize the convex hull property to a more explicit statement. We use hyperbolic planes as barrier surfaces and obtain C^0 bounds in terms of the domain Ω and the boundary curve Γ.

In the following we use two different measures for the distance of two closed bounded sets K and L in a metrical space Ω. Let $p \in K$, then we have

$$dist(p, L) := \min_{q \in L} dist(p, q)$$

where $dist(p, q)$ is the distance of points in Ω. With this, we define

$$dist(K, L) := \min_{p \in K} dist(p, L)$$
and
$$DIST(K, L) := \max_{p \in K} dist(p, L).$$

$dist(p, L)$ specifies the shortest distance between points of K and L, whereas $DIST(K, L)$ is the longest distance between points of K to the set L. In general, $DIST$ is not symmetric in its arguments.

Lemma 12. *Let $\Omega \subset \mathbf{C}$ be a bounded domain in the UHM^3, $K \subset\subset \overset{\circ}{\Omega}$ a compactum and $f : \Omega \longrightarrow \mathbf{R}$ a minimal graph over Ω with boundary $\Gamma : \partial\Omega \longrightarrow [0, G] \subset \mathbf{R}$ with constant $0 \leq G < \infty$. Then there exist constants*

$$C_1(\Omega, K) := dist(K, \partial\Omega) \text{ and}$$
$$C_2(\Omega, \Gamma) := \sqrt{G^2 + \tfrac{1}{4} diam^2 \Omega}$$
such that
$$\forall z \in K : \ 0 < C_1(\Omega, k) \leq f(z) \leq C_2(\Omega, \Gamma) < \infty.$$

Proof. . By the convex hull principle 8, a minimal surface in H^3 will lie on one side of a hyperbolic plane as long as its boundary does. Let $p \in K$ and consider an "infinitesimal" hyperbolic plane, i.e. a small Euclidean halfsphere in the UHM with center p. Γ and therefore $f(\Omega)$ will lie on one side of the sphere as long as its Euclidean radius is less then $dist(K, \partial\Omega)$. This proves the lower bound.

To get an upper bound we argue in a similar way using a barrier sphere from above: the cylinder $\partial\Omega \times [0, G]$ can be covered by a halfsphere of radius bigger than $\sqrt{G^2 + \frac{1}{4} diam^2 \Omega}$.

The estimate of lemma 12 remains true, if f is not a graph. Let f be a minimal surface with given boundary Γ, Γ defined as in the lemma as the boundary of a bounded domain Ω. The projection of f may cover a larger set Ω' containing Ω and f being multivalued on Ω'. Let $K \subset \mathbf{C}$ a compactum with $K \cap \partial\Omega = \emptyset$, then the estimates of lemma 12 hold with the same constants.

Lemma 12 gives a rough estimate of f since e.g. C_2 is a global estimate of f over Ω. The following lemma gives a better estimate by taking into account the trigonometry of the barrier spheres.

Lemma 13. *Let $\Omega \subset \mathbf{C}$ be a bounded strictly convex domain in the UHM, $K \subset\subset \overset{\circ}{\Omega}$ a compactum and $f : \Omega \longrightarrow \mathbf{R}$ a minimal graph over Ω with boundary $\Gamma : \partial\Omega \longrightarrow [G_1, G_2] \subset \mathbf{R}$ with constants $0 \leq G_1 \leq G_2 < \infty$. Denote with $\kappa_{\min}$ the euclidean minimal curvature of Γ. Then there exist constants*

$$C_1(\Omega, K, \Gamma) = \sqrt{G_1^2 + dist^2(K, \partial\Omega)}$$
$$C_2(\Omega, K, \Gamma) = \sqrt{G_2^2 + DIST(K, \partial\Omega) \cdot (\tfrac{2}{\kappa_{\min}} - DIST(K, \partial\Omega))}$$
such that
$$\forall z \in K : \ 0 < C_1(\Omega, K, \Gamma) \leq f(z) \leq C_2(\Omega, K, \Gamma) < \infty.$$

Proof. . Let $q \in \Omega$ an interior point and $q' \in \Gamma$ a point which has minimal distance to q. Let L denote lifting by G_2 in the vertical direction. Then $L(\partial\Omega)$ lies above Γ. We can cover $L(\partial\Omega)$ by a Euclidean halfsphere which is tangent to $L(\partial\Omega)$ at $L(q')$ and whose circle of latitude through $L(q')$ at height C_2 has curvature $\frac{1}{\kappa_{\min}}$. From this we immediately obtain the constant C_2.

Chapter 4

A Priori Gradient Estimates

In this chapter we will prove a priori gradient estimates at interior points of minimal surfaces in H^3 in terms of their boundary. The surfaces must be bounded and of disk type, but we do not assume them to be given as graphs. We will argue geometrically and get a priori estimates by restricting the set of possible directions of the normal vector at interior points of the surface.

Our method originates in T. Rado's "four point condition" and uses ideas from Lawson's generalization [20] to minimal surfaces with boundary in S^3. The corresponding "Hyperbolic Four Point Condition" is a special case of our theorem 17: Given a simply connected non planar minimal surface with boundary, then the intersection of each tangent plane with the boundary consists of at least four different components.

Reversing the implication of the statement we can exclude all totally geodesic planes with less than four disjoint components in common with the boundary from being tangent to the surface somewhere.

We use the hyperbolic four point condition to prove our main gradient estimates in theorems 18 and 19. The estimates are valid for minimal surfaces with boundary contours satisfying a certain convexity property. The theorems do not assume that the surfaces are given as graphs. This will be proved. For contours with such a convexity property uniqueness of the minimal surface is not known and is false in general.

In theorem 20 we prove an additional estimate for minimal graphs over strictly convex domains.

4.1. A Sub/Super Harmonic Function

In the following we let

$$F : M^2 \to H^3 \subset \mathbf{R}^4_L$$

be a conformal non planar minimal immersion of a simply connected Riemannian surface M with boundary ∂M into hyperbolic space H^3.It is a essential condition that H^3 is embedded in an ambient space with vector space structure. For convenience we work with a compact $M \subset \mathbf{C}$.

We assume further that F is regular and real analytic in the interior and that no interior branch points occur. If F is a Morrey solution to a Plateau problem

these assumptions are fulfilled by Morrey [25] and Gulliver [9]

Lemma 14. *Let F be a minimal surface as above with local coordinates u and v. Then*

$$\triangle F = 2\lambda \cdot F, \tag{4.1}$$

where $\triangle = \frac{\partial^2}{\partial u^2} + \frac{\partial^2}{\partial v^2}$ is the Laplace operator of the Euclidean metric in the domain and λ is the conformal factor of the induced metric.

Proof. . The relation follows immediately from the Frobenius system for hyperbolic surfaces 2.2.

We will now define a function on M which is sub or super harmonic on well defined regions. In Euclidean space such a function could be immediately obtained since all coordinate functions of a conformal minimal immersion are harmonic. We adapt here a construction used by Lawson in S^3. It depends heavily on the embedding of H^3 into the vector space structure of $\mathbf{R}^4_L$. Let P be a totally geodesic plane of H^3 in $\mathbf{R}^4_L$ and let $N_P \in \mathbf{R}^4_L$ be one of its two normal vectors. By section 1.1.7 the normal vector to a specific plane does not depend on the base point. The plane P can now be written as

$$P = \left\{ p \in H^3 \mid \langle p, N_P \rangle_L = 0 \right\}.$$

From these remarks we can define a real valued function f_P on M by

$$f_P := \langle N_P, F \rangle_L : M \to \mathbf{R}. \tag{4.2}$$

The following lemma shows that this function can be used as a substitute for the harmonic functions available in Euclidean space.

Lemma 15. *Let $F : M \to H^3 \subset \mathbf{R}^4_L$ be a minimal surface, P a totally geodesic plane and f_P the function defined above. Then f_P is super resp. sub harmonic in open connected sets where $f_P \geq 0$ resp. $f_P \leq 0$, and therefore satisfies a sharp maximum resp. minimum principle.*

Proof. . Sub resp. super harmonicity of f_P follows directly by applying the Laplace operator $\triangle$ to the defining equation 4.2. Since N_P and $\langle ., . \rangle_L$ are parallel with respect to $\triangle$ we obtain by using lemma 14

$$\triangle f_P = \langle N_P, \triangle F \rangle_L = 2\lambda \cdot f_P \ . \tag{4.3}$$

1.)Since the sign of f_P depends on the choice of the direction of N_P the application of the maximum principle of lemma 15 is independent of the sign of f in a domain of interest.

2.)The comparable equation to 4.1 in S^3 has a different sign. This has greater effect than just changing sign in all equations in H^3. In H^3 we have $f_P \geq 0 \Rightarrow$ maximum principle, while in S^3 we have $f_P \leq 0 \Rightarrow$ minimum principle. This leads to two different situations, whose non-existence is proved by using lemma 15 (see figure 15).

4.2. Hyperbolic Rado's Lemma

After this preparatory discussions we will now extend Rado's ideas to minimal surfaces in H^3. The following lemma 16 and theorem 17 are generalized from Lawson [20] to H^3.

Lemma 16. *Let $C := \psi^{-1}(P)$ be the preimage of the intersection of $\psi(M)$ with a totally geodesic plane P. Then for every component $\mathcal{O}$ of $\overset{\circ}{M} \setminus C$, the set $\partial\mathcal{O} \cap \partial M$ must contain an interval.*

Proof. . The proof works by a contradiction to the maximum principle. Let N_P be the unique normal vector of P, such that

$$P = \left\{ x \in H^3 \mid \langle N_P, x \rangle_L = 0 \right\}$$

and let f_P be defined by

$$f_P := \langle N_P, . \rangle_L .$$

A component $\mathcal{O}$ of $\overset{\circ}{M} \setminus C$ is then a component of

$$\left\{ x \in \overset{\circ}{M} |\ f_P(x) > 0 \right\} \text{ or } \left\{ x \in \overset{\circ}{M} |\ f_P(x) < 0 \right\}.$$

We assume $f_{P|\mathcal{O}} > 0$. Along $\partial\mathcal{O} \cap \overset{\circ}{M}$ f_P clearly vanishes. Therefore, if $\partial\mathcal{O} \cap \partial M = \emptyset$ or $f_{P|\partial\mathcal{O}\cap\partial M} \equiv 0$ then $f_{P|\mathcal{O}}$ has an interior maximum in contradiction to the maximum principle of lemma 15. It follows that there exists a $p \in \partial\mathcal{O} \cap \partial M$ with $f_P(p) > 0$. By continuity, $f_P > 0$ in some neighbourhood U of p. Since ψ is continuous at the boundary $\partial M \cap \partial\mathcal{O} \supset \partial M \cap \partial U$ contains an interval.

The following theorem is a generalization of a well known lemma of Rado and its spherical version of Lawson. Rado proved his theorem for harmonic functions on the unit disk (compare e.g. [5]). A special case of theorem 17 is the "Hyperbolic Four Point Condition" mentioned in the introduction of this chapter. The theorem is an essential ingredient for our later gradient estimates.

Theorem 17 [Hyperbolic Rado's lemma]**.** *Let $\psi(M)$ be a non planar minimal immersion of disk type with boundary in H^3. If a totally geodesic plane P has k-th order of contact with $\psi(M)$ at a point $p \in \overset{\circ}{M}$, then $\psi^{-1}(p) \cap \partial M$ has at least $2(k+1)$ components.*

Proof. . Let N_P be a normal vector of P. Then we can introduce a height function $f := \langle N_P, \psi \rangle_L$ as in equation 4.2. In local coordinates (u, v) for M with center p is real analytic and its power series expansion about p is given by

$$f(u, v) = \sum_{i=0}^{\infty} p_i(u, v)$$

with homogeneous polynomials p_i of degree i. By the assumption we have that $p_0 = ... = p_k = 0$. Let p_{l+1} be the first non vanishing polynomial. Since $\psi(M)$ is minimal, equation 4.3 gives $\triangle f = 2\lambda f$. Therefore $\triangle p_{l+1} = 0$ and p_{l+1} is the real part of a holomorphic polynomial of degree $l+1$:

$$\begin{aligned} p_{l+1} &= c \cdot Re(e^{i\theta} \cdot w^{l+1}) \\ &= c \cdot (\cos\theta \cdot Re(w^{l+1}) - \sin\theta \cdot Im(w^{l+1})) \end{aligned}$$

where $w = u + iv$ and c, θ are constants. Consequently $\psi^{-1}(p)$ divides a neighbourhood of p into $2l+2$ open sectors such that f changes sign between two adjacent sectors. Using the maximum principle one easily shows that no two sectors can coincide. With the help of lemma 16 and because M is of disk type it follows that $\overset{\circ}{M} \setminus \psi^{-1}(p)$ and $\partial M \setminus \psi^{-1}(p)$ must have at least $2l+2$ components.

4.3. Gradient Estimates

An important application of our Hyperbolic Rado's Lemma is the following statement of embeddedness:

Theorem 18. *Let M be a minimal surface of disk type with boundary $\Gamma \subset H^3$. Suppose there exists a geodesic fibration of H^3 induced by a p-coordinate system with center $p \in S^\infty$ such that the projection π along the fibers maps Γ 1 − 1 onto the boundary of a p-convex set in S^∞. Suppose further that for all $p \in \Gamma$ the fiber through p intersects T_pM and is not tangent. Then*

a) $\forall p \in M$ *the surface normal is not orthogonal to the fiber through* p
a′) $\forall p \in M$ *the tangent plane T_pM does not contain the fiber through* p
b) M *is embedded.*

Proof. . The statements a and a′ are obviously equivalent. We prove a′. Suppose there exists a point $p \in M$ with T_pM containing the fiber through p. By theorem 17 $T_pM \cap \Gamma$ and therefore $T_pM \cap \pi(\Gamma)$ consists of at least four components. This contradicts the fact that $\pi(\Gamma)$ is convex. This proves a′.

Suppose M is not embedded. Then there exists a fiber having at least two intersection points with M. Because M is embedded along Γ and projects 1-1 along a neighbourhood of Γ, from the regularity of M follows the existence of a point $p \in M$, where the fiber through p is contained in T_pM. This contradicts a′.

The following theorem states our main gradient estimate. The estimates on the normal vector are also gradient estimates for the hyperbolic minimal surface equation 2.1. Since the equation is singular at the infinite part of the boundary, such results do not directly follow from elliptic theory. The proof is based on our Hyperbolic Rado's Lemma.

Theorem 19. *Let $p_0 \in S^\infty$ with open neighbourhood $B \subset S^\infty$ such that ∂B is a spherical circle with center p_0. Let $\Gamma \subset H^3$ be a Jordan curve which has $\forall$ $p \in B$ a 1-1 p-projection on a p-convex curves in S^∞. If M is a minimal surface bounded by Γ, then M is a graph and the angle α between the normal at a point $q \in M$ and the p_0-geodesic through q is bounded from above by*

$$\alpha(q) \leq \arctan(\sinh dist(q, C(B))) =: \alpha_{\max}(q),$$

where $C(B)$ is the convex hull of B.

If $M' \subset M$ is a compact subset of M, then the normals at points of M' are uniformly bounded by

$$\alpha_{|M'} \leq \arctan(\sinh(\max_{q' \in M'} dist(q', C(B)))) =: \alpha_{\max}(M').$$

Writing M as a graph $f : \Omega \to \mathbf{R}$ the above bound is equivalent to a C^1-bound for f:

$$\left| grad\, f_{|q} \right| = \tan \alpha(q) \leq \sinh dist(q, C(B)).$$

Proof. . For a fixed point $q \in M$ the geodesic through q and points of B form a solid cone which has an opening angle ψ given by lemma 2

$$\cot \frac{\psi}{2} = \sinh dist(q, C(B)),$$

where $C(B)$ denotes the convex hull of B. Because of the projection property of Γ we can apply corollary 18. Therefore no geodesic of the cone through q can be tangent to M in q. Together with the value of the cone angle ψ we obtain an upper bound $\alpha_{\max}(q)$ for the angle of the normal at q with the p_0-geodesic by

$$\alpha_{\max}(q) = \frac{\pi}{2} - \frac{\psi}{2}.$$

This proves the theorem.

We consider now a minimal surface with strictly convex boundary curve on $\mathbf{C}$ in the UHM. We obtain an explicit gradient estimate by purely geometric reasoning for the hyperbolic minimal surface equation. The situation with $\Gamma \subset S^\infty$is much easier to handle than the situation $\Gamma \subset S^\infty \cup H^3$ since one can use translated copies of the minimal surface as barriers. Compare theorem 24.

Lemma 20. *Let $\Gamma \subset \mathbf{C} \subset S^\infty$ be a strictly convex curve in the upper half space model bounding a domain $\Omega \subset \mathbf{C}$. Further let M be a minimal surface with asymptotic boundary Γ and p a point on M. Denote with q the vertical projection of p onto Ω and with $\kappa_{\min}$ the minimal curvature of Γ as a Euclidean curve.*

Then M is a graph and the angle α of the normal N_p at p with the vertical direction is bounded above as follows:

$$\alpha(p) \leq \arccos(dist(q,\Gamma)\cdot\kappa_{\min}).$$

Writing M as a graph $u:\Omega\to\mathbf{R}$, this bound is equivalent to a C^1 bound for u :

$$\left|grad\ u_{|q}\right| = \tan\alpha(p) \leq \frac{\sqrt{1-dist^2(q,\Gamma)\cdot\kappa_{\min}^2}}{dist(q,\Gamma)\cdot\kappa_{\min}}.$$

The estimate is sharp for circular domains, i.e.

$$\left|grad\ u_{|q}\right| = \frac{\sqrt{1-dist^2(q,\Gamma)\cdot\kappa_{\min}^2}}{dist(q,\Gamma)\cdot\kappa_{\min}}, q\in\Omega.$$

Proof. . Assume there exists a point $p\in M$, whose normal N_p encloses an angle $\alpha > \alpha_{\max} := \arccos(dist(q,\Gamma)\cdot\kappa_{\min})$. We will show that then a one parameter family of minimal surfaces M_t with boundaries $\Gamma_t\subset S^\infty$ exists, obtained by parallel translation of M along a hyperbolic geodesic γ through p such that all Γ_t are disjoint, and that there exist t_0, t_1 with $M_{t_0}\cap M_{t_1}\neq\emptyset$. In such a situation a standard argument applies: fix t_0 and move a copy of M_{t_0} along γ until both surfaces are disjoint. Then move the copy back until both surfaces meet the first time. Since the boundaries are disjoint, both surfaces have tangential contact at an interior point contrary to the maximum principle.

Let T_pM be the tangential plane of a point $p\in M$, whose normal in p encloses an angle $\alpha > \alpha_{\max}$ with the vertical direction. We denote with q' the closest point of $T_pM\cap S^\infty$ to p in the Euclidean metric of $\mathbf{C}$. Further let $\gamma'\subset T_pM$ be a hyperbolic geodesic containing p and q' and enclosing with the vertical direction in p an angle $\frac{\pi}{2}-\alpha$. Then the bound $\alpha_{\max}$ ensures that γ' is part of a Euclidean circle with radius $r > \frac{1}{\kappa_{\min}}$: Let h be the Euclidean height of p over $\mathbf{C}$ and $\delta = dist(q,\Gamma)$. Then, using the inequality $\alpha > \alpha_{\max}$ and the lower C^0 estimate for h (see lemma 12), we have

$$r = \frac{h}{\cos\alpha} > \frac{h}{\cos\alpha_{\max}} = \frac{h}{\delta\cdot\kappa_{\min}} \geq \frac{1}{\kappa_{\min}}\ . \tag{4.4}$$

Additionally, the inequality $\alpha > \alpha_{\max}$ ensures that one end point of γ' lies inside the neighbourhood $U_\delta(q)\subset\Omega$. Let $q'\in\mathbf{C}$ be the end point of γ' closest to q.

Then using the Euclidean distance we have:

$$\begin{aligned} dist(q,q') &= r - \sqrt{r^2 - h^2} \\ &\leq \tfrac{1}{\kappa_{\min}} - \sqrt{\tfrac{1}{\kappa_{\min}^2} - h^2} \\ &\leq \tfrac{1}{\kappa_{\min}} - \sqrt{\tfrac{1}{\kappa_{\min}^2} - h_{\max}^2} \\ &= dist(q,\Gamma) = \delta. \end{aligned}$$

The first inequality is true since the function is strictly decreasing in r and we have by equation 4.4 a lower bound for r. For the second inequality we estimate h from above by the upper C^0 bound $h_{\max} := C_2 = \sqrt{dist(q,\Gamma)(\frac{2}{\kappa_{\min}} - dist(q,\Gamma))}$ of lemma 13, from which we immediately obtain the result.

We have now proved that the endpoints of γ' lie on both sides of M. Since γ' is tangential to M we can find a geodesic γ close to γ' in the Euclidean metric, which starts in $U_\delta(q)$, has radius $r > \frac{1}{\kappa_{\min}}$ and intersects M at least two times in interior points p_1 and p_2. We now parallel translate M along γ in direction away from q. Then each trajectory of a point of Γ is a circular arc in $\mathbf{C}$ with radius greater than $\frac{1}{\kappa_{\min}}$ starting close to q. Therefore the trajectories intersect Γ exactly once, and all parallel translated copies of Γ are mutually disjoint. On the other hand there exist numbers $t_0 \neq t_1$ with $M_{t_0} \cap M_{t_1} \neq \emptyset$. Using the standard argument from the beginning of the proof we have a contradiction to the maximum principle.

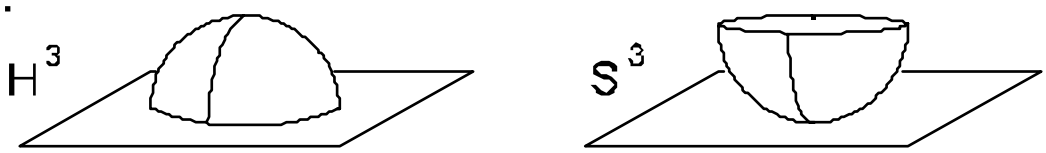

Figure 4.1: Difference of Maximum Principle between H^3 and S^3

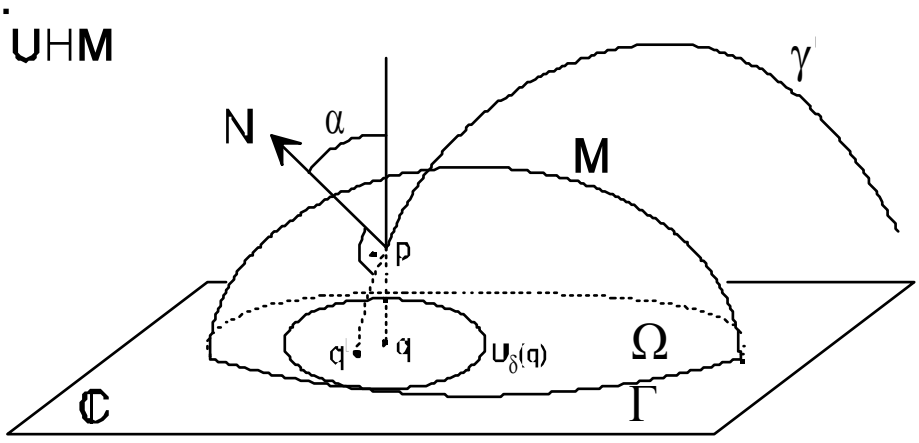

Figure 4.2: Estimate of Angle Between Surface Normal and Geodesic Fibration

Chapter 5

Existence and Uniqueness

In this chapter we prove a new existence theorem (theorem 29) for disk type minimal surfaces bounded by a given Jordan curve Γ. It is the first theorem which allows the boundary Γ to lie in part in the interior of H^3 as well as on the infinite boundary S^∞ of H^3. In some sense our theorem generalizes the famous existence theorem of Jenkins and Serrin for minimal surfaces in $\mathbf{R}^3$ (see theorem 27 below) who solved the Euclidean minimal surface equation for a boundary contour consisting of finite and infinite segments. In contrast to the Euclidean case, the infinite parts of the boundary contour may be much more general in hyperbolic space. This effect was expected from the existence proofs of Anderson (see theorems 21 and 22).

We make the a priori assumption on Γ that there exists a small open neighbourhood $B \subset S^\infty$ such that for all $p \in B \subset S^\infty$ Γ possesses a 1-1 p-projection onto a p-convex curve in S^∞ along the fibration of H^3 induced by geodesics through p. The term p-convex was introduced in definition 11. In the corresponding UHM with $p = \infty$ the p-convex curves correspond to Euclidean convex curves in the complex plane $\mathbf{C} \subset S^\infty$ which need not be strictly convex. In fact, if Γ contains a geodesic arc the projected boundary may be non-strictly convex in $\mathbf{C}$ for all $p \in B$. In our proof we construct a minimizing sequence using a priori estimates for the gradient derived using mainly geometric terms. The estimates rely on the results of chapter 4.

There exists a long sequence of different existence theorems for Plateau problems in minimal surface theory. In the famous work of Douglas [6] and Rado [31] around 1930 both proved simultaneously the existence of an area minimizing disk in an arbitrary Euclidean Jordan curve. This was generalized several years later by Morrey [25] to arbitrary ambient Riemannian manifolds with homogeneously regular metric, i.e. the ambient manifold does not behave too pathological at infinity. In the meantime A.T. Lonseth [23], a student of H. Lewy, proved in 1942 the existence of area minimizing disks in hyperbolic space H^3. Lonseth was the first to put special focus on hyperbolic minimal surfaces. In 1982 Anderson [1], [2] proved existence of a large class of minimal surfaces in H^3 whose boundary lies in the asymptotic sphere S^∞ of H^3.

Theorem 21 [Anderson 1]. *Let $\Gamma \subset S^\infty$ be an immersed closed Jordan curve. Then there exists a complete, smoothly embedded minimal disk Σ in H^3 with asymptotic boundary Γ at S^∞. Σ is area minimizing in the category of embedded disks.*

Sketch of the proof: Let $\Gamma \subset S^\infty$ be a smooth curve and $p \in C(\Gamma)$ a point in the convex hull of Γ. We retract Γ smoothly to p via the geodesic flow and let

$$\Gamma_t = \{\gamma_q(t) \mid \gamma_q \text{ the unit speed geodesic from } p \text{ to } q \in \Gamma\}$$

solve the Plateau problem for the sequence of finite boundaries Γ_t. To prove convergence of a subsequence it is necessary and sufficient to find bounds $c_r, C_r > 0$ such that for all $r \geq R_0$ the mass $\underline{M}(\mathrm{M}_t \lfloor B_r)$ of a minimizing integral p-current M_t with $\partial \mathrm{M}_t = \Gamma_t$ inside balls B_r of radius r is bounded by

$$c_r \leq \underline{M}(M_t \lfloor B_r) \leq C_r.$$

c_r and C_r are constants depending only on r. These estimates are based on a monotonicity formula for the volume growth of stationary currents in geodesic balls and on the behavior of convex sets in H^3 in the large.

In fact, Anderson's results are more general as he allows the ambient manifold to be H^n and the minimizing varieties to be of any codimension. His proofs are in the setting of geometric measure theory.

The following theorem Anderson [2] considers minimal graphs in the upper halfspace model defined over a convex domain $\Omega \subset \mathbf{C}$:

$$f : \Omega \subset \mathbf{C} \to \mathbf{R}$$
$$f_{|\partial\Omega =: \Gamma} = 0.$$

Theorem 22 [Anderson 2]. *Let $\Gamma \subset S^\infty$ be a convex curve in the upper half space model such that $\Gamma \subset \mathbf{C}$. Then there exists a unique minimal graph M which is complete and absolutely area minimizing with asymptotic boundary Γ.*

Anderson's proof uses elliptic theory for the hyperbolic minimal surface equation 2.1 but he does not mention C^1 estimates. Using our lemma 19 we obtain explicit C^1 estimates. The situation with $\Gamma \subset S^\infty$is much easier to handle than the situation $\Gamma \subset S^\infty \cup H^3$ since one can use translated copies of the minimal surface as barriers. Compare theorem 24 below.

Hardt and Lin [10] and Lin [22] proved the following theorem in H^n which we state for H^3. For the existence part they used Anderson [2].

Theorem 23 [Hardt/Lin 1]. *Suppose $\Omega \subset \mathbf{C}$ is star-shaped with respect to a point $q \in \Omega$. Then there exists a unique area minimizing surface M with asymptotic boundary $\partial\Omega$. Moreover M is a graph over a halfsphere with center q.*

Lin [22] proved the graph property of the minimal surface M of theorem 23 by using a Steiner type symmetrization. In H^3 we can see this property more directly, as well as the uniqueness statement of Anderson's theorem 22, by using the maximum principle:

Theorem 24. *Let $\Gamma \subset S^\infty$ be the boundary of a minimal surface M. If there exists a hyperbolic translation, such that the corresponding orbits on S^∞ are transversal to Γ, then M is unique and a graph over hyperbolic planes orthogonal to the axis of translation.*

Proof. . In the most general case Γ may be star-shaped w.r.t. a point $q \in S^\infty$. We choose the axis of a translation T to emanate from q and end in the other component of S^∞ not including q. Since Ω is star-shaped w.r.t. q all translations of $\partial\Omega$ under T will be disjoint. Therefore if a Euclidean straight line through q intersects M more than once, we can translate a copy M' of M such that $M' \cap M = \emptyset$. Then we move M' back until it first meets M at an interior point contradicting the maximum principle. This proves that M is the unique minimal surface bounded by $\partial\Omega$ and a graph w.r.t. the fibration of H^3 induced by T.

Hardt and Lin [10] and Lin [22] proved boundary regularity at infinity for the area-minimizing surfaces with boundary in infinity obtained by Anderson:

Theorem 25 [Hardt/Lin 2]**.** *Consider H^3 represented as PM^3, KM^3 or UHM^3. For any area-minimizing surface $M \subset H^3$ with asymptotic boundary $\Gamma \subset C^{1,\alpha}$, $0 < \alpha \leq 1$, the set $M \cup \Gamma$ is, near Γ, a finite union of $C^{1,\alpha}$ submanifolds with boundary Γ in the Euclidean metric. They meet S^∞ orthogonally at Γ.*

In Polthier [29] we solved free boundary value problems for minimal surfaces in H^3 by using a conjugate surface construction. Consider a (p, q, r) Coxeter orthoscheme with $p, q, r \in \mathbf{N}$ as they occur in tessellations of H^3. These are specific tetrahedrons whose vertices (P_1, P_2, P_3, P_4) have the property that $span(P_1, P_i) \perp span(P_i, P_4)$ for $i \in \{2, 3\}$ and whose dihedral angles are of the form $\frac{\pi}{2}, \frac{\pi}{2}, \frac{\pi}{2}, \frac{\pi}{p}, \frac{\pi}{q}, \frac{\pi}{r}$. We proved existence of a minimal patch with four free boundary curves, each lying on a face of the tetrahedron, for the following class of Coxeter orthoschemes:

Theorem 26 [Triply Periodic Surfaces]**.** *There exist complete minimal surfaces in H^3 with the symmetry of tessellations given by*

- *all compact and non-compact platonic solids*
- *all Coxeter orthoscheme (p, q, r) with $q \in \{3, 4, ..., 1000\}$ and small p and r*

- *all selfdual Coxeter orthoscheme with $p = q$, and additionally all rotational symmetric Coxeter orthoscheme with all four vertices in or beyond infinity (their Coxeter graph is $0 \cdots 0 \overset{n}{-} 0 \cdots 0$, they have no (p, q, r) representation).*

For the existence proof we used the conjugate surface construction. We proved existence of a quadrilateral contour in a two parameter family of candidates, such that the conjugate of the minimal patch in the quadrilateral is bounded by a Coxeter orthoscheme. See figure 8.10 for a minimal cell in a hyperbolic 60°-cube.

The following existence theorem of Jenkins and Serrin [12] is powerful for the construction of simply and doubly periodic minimal surfaces in $\mathbf{R}^3$ (see e.g. Karcher [14] and [17]). They considered boundary configurations in Euclidean space $\mathbf{R}^3$ which arise in the following way when trying to generalize Scherk's first surface: start with a convex planar polygon in the (x, y)-plane and assign to each edge of the polygon a constant height value. The constant may be a real number as well as plus or minus infinity. At vertices, vertical lines are used to connect two adjacent edges of different height. Jenkins and Serrin gave necessary and sufficient criteria for such Jenkins-Serrin contours to bound an embedded, unique minimal surface which is a graph except for the vertical boundary segments. The existence proof heavily uses the first surface of Scherk as a barrier for a minimizing sequence and good knowledge of the conjugate function to the graph function $f(x, y)$:

Theorem 27 [Jenkins/Serrin]**.** *In the Dirichlet problem stated above we denote open arcs of the polygon P with finite height as $C_1, C_2, .., C_m$, arcs with plus resp. minus infinity as $A_1, .., A_k$ resp. $B_1, .., B_l$. Let α resp. β denote the total length of the segments A_i resp. B_i and let γ denote the perimeter of the polygon. Then, if the family $\{C_i\}$ is not empty, the Dirichlet problem has a solution if and only if*

$$2 \cdot \alpha < \gamma \text{ and } 2 \cdot \beta < \gamma \ .$$

If $\{C_i\}$ is empty the condition has to be replaced by $\alpha = \beta$. The solution is unique and a graph over the interior of p.

The following definitions will help us talk about the geometric setting of our main existence theorem in this chapter. We have chosen an intrinsic formulation since we frequently change among upper halfspace models.

Definition 28.

- *A* **p-horosphere** *is a horosphere in H^3 with center p.*
- *A* **p-geodesic** *is a hyperbolic geodesic through p.*
- *A* **p-coordinate system** *of H^3 is given by the fibration induced by all p-geodesics and all p-horospheres. This is equivalent to a specific UHM of H^3, where p lies in ∞. The p-geodesics then become fibres $\{z\} \times \mathbf{R}^+$, $z \in \mathbf{C}$, and the p-horospheres become Euclidean planes parallel to $\mathbf{C}$.*

- *A surface is a* **p-graph** $\Longleftrightarrow$ *every p-geodesic intersects the surface at most once. Minimal p-graphs fulfill the hyperbolic minimal surface equation 2.1.*

- *The normals of an oriented surface are* **p-bounded** *by an angle* $\alpha :\Leftrightarrow$ *at every point q on the surface the angle between the surface normal and the p-geodesic through q is less than* α.

- **p-projection** *is projection of points along p-geodesics onto* S^∞.

- *A* **p-convex** *set* $\Omega \subset S^\infty$ *was defined in definition 11*

We will now state our main existence theorem which proves existence of an embedded minimal disk bounded by a contour lying in part in the interior of H^3 and in part on the asymptotic boundary S^∞.

Theorem 29 [Existence Theorem]**.** *Let* $\Gamma \subset H^3 \cup S^\infty$ *be a Jordan curve and let* $B \subset S^\infty$ *be an open set such that* $\forall p \in B$ *the curve* Γ *p-projects 1-1 onto the boundary of a p-convex set in* S^∞.

Then there exists an embedded minimal disk M with boundary Γ. *For all* $p \in B$ *M is a p-graph.*

- I was informed by Burago, that Schefel [32] proved a compactness theorem for saddle surfaces in $\mathbf{R}^3$, i.e. surfaces with non-positive Gauß curvature, which appears to be similar in spirit. But his arguments were not detailed.

- Contrary to the Euclidean case we need no balancing condition on the ends as in the theorem 27 of Jenkins and Serrin.

- The requirement of an open set B of projection centers has technical reasons to ensure the gradient estimates. In contrast to Euclidean space we have no uniqueness of a minimal graphs with finite or mixed boundary contour defined over a convex domain in the UHM.

- The projection property of Γ is not equivalent to the existence of a $p_0 \in S^\infty$ such that Γ p_0-projects onto a strictly convex curve in S^∞. If Γ for example contains a geodesic arc, this arc will project to a Euclidean straight arc in $\mathbf{C}$ for all $p \in B$, i.e. p-projection(Γ) will be non-strictly convex for all $p \in B$.

- The results of Hardt and Lin about the asymptotic regularity at infinity do not apply directly since they assume $\partial M \subset S^\infty$ and also M being area-minimizing.

Proof. . We construct a sequence of finite minimal disks as Morrey solutions to finite contours. Using the results of chapters 3 and 4 we obtain a priori $\mathbf{C}^0$ and $\mathbf{C}^1$ estimates, and then use elliptic theory for the minimal surface equation 2.1 to obtain a minimal surface as a limit. For the proof we fix an arbitrary point $p_0 \in B$ and use the $p_0 - UHM$ as a coordinate system. Let Ω be the interior of p_0-projection(Γ) onto $\mathbf{C}$ and the curve Γ be given as a function on $\partial\Omega$:

$$\Gamma : \partial\Omega \longrightarrow \mathbf{R}.$$

We define a sequence of finite curves $\{\Gamma_n\}$ on $\partial\Omega$ by

$$\Gamma_n : \partial\Omega \longrightarrow \mathbf{R}$$
$$\Gamma_n(z \in \partial\Omega) = \begin{cases} \Gamma(z) & \text{if } \Gamma(z) \geq \frac{1}{n} \\ \frac{1}{n} & \text{else.} \end{cases}$$

For n large enough, this results in clipping the infinite part of Γ at a horosphere. The sequence $\{\Gamma_n\}$ converges uniformly to Γ w.r.t. the Euclidean metric. Since by the p-convexity assumption on Γ the infinite segments of Γ have to be strictly convex arcs in the $p_0 - UHM$ (this is only true for the infinite segments, compare the remark to the theorem). Therefore the convexity properties of Γ carry over to all Γ_n.

Let $\{f_n\}$ be a sequence of area minimizing Morrey solutions bounded by the finite contours $\{\Gamma_n\}$ and let $\Omega' \subset\subset \Omega$ be a compact subset in Ω. Let $f_{n|\Omega'}$ denote the set of f_n lying above Ω' (we have not yet proved that f_n is a graph). We apply lemma 12 (compare the remark following lemma 12) to all minimal surfaces f_n and obtain constants

$$C_1(\Omega, \Omega') := dist(\partial\Omega, \Omega'),\ C_2(\Omega, \Gamma) := \sqrt{\max_{z\in\partial\Omega} \Gamma(z)^2 + \frac{1}{4} diam^2\Omega}$$

such that for all n graph $f_{n|\Omega'}$ is uniformly bounded by

$$0 < C_1(\Omega, \Omega') \leq f_{n|\Omega'} \leq C_2(\Omega, \Gamma) < \infty.$$

Uniform gradient estimates for $f_{n|\Omega'}$. W.l.o.g. we assume ∂B is a spherical circle. Since all minimal surfaces $\{f_n\}$ have the same projection property, we can apply theorem 19 and obtain uniform gradient bounds for the sequence $\left\{f_{n|\Omega'}\right\}$. By the previous established uniform lower C^0 bound $C_1(\Omega, \Omega')$ we can get a uniform upper bound $r_{\max}$ for the distance r of points on $\left\{f_{n|\Omega'}\right\}$ to the convex hull $C(B)$ of B:

$$r_{\max} = \max_{q\in\Omega'\times\left\{C_1(\Omega,\Omega')\right\}} dist(q, C(B)).$$

Using theorem 19 we obtain a uniform upper bound for the gradient of $\left\{f_{n|\Omega'}\right\}$ above Ω':

$$\left|grad(f_{n|\Omega'})\right| \leq \sinh r_{\max} =: C(\Omega, \Omega', B).$$

We additionally note the uniform upper bound of the angle α of the normals with the vertical direction:

$$\alpha(q) \leq \arctan(\sinh r_{\max}),\ \forall n \in \mathbf{N},\ \mathrm{q} \in f_{n|\Omega'}.$$

We can now apply standard elliptic theory as e.g. we can use theorem 13.3 of Gilbarg and Trudinger [8] showing that $\left\{f_{n|K}\right\}$ satisfies a strictly elliptic equation with Hölder continuous derivatives on compact subsets $K \subset\subset \Omega$. Further using corollary 6.3 of [8] we get uniform bounds for $\left\{|f_n|_{2,\alpha;K}\right\}$ with $\alpha > 0$ on compact subsets $K' \subset\subset K$.

$\{f_n\}$, $\{Df_n\}$ and $\{D^2 f_n\}$ are therefore equicontinuous and uniformly bounded on a compact subset K' and contain by Arzela/Ascoli a subsequence which converges uniformly in $C^2(K')$ to a minimal surface over K'.

We now use a standard diagonal argument to prove existence of a limit minimal surface over Ω. Let $\{K_n\}$ be a sequence of compact sets exhausting Ω with $K_n \subset K_m$ for $n < m$. Starting with the original sequence $\{f_n\}$ of Morrey solutions we obtain a subsequence $\left\{f_{n_{(1)}}\right\}$ by the above process converging to a minimal surface M_1 on K_1. Iterating this process on all subsets K_i and using a diagonal argument we obtain a sequence of minimal surfaces, we call them $\{f_n\}$ again, converging to some f in the C^2 topology on compact sets. The boundary behavior on the finite part of Γ is controlled by the hyperbolic $p-$planes through Γ, which are barriers for all finite Morrey solutions along $\partial\Omega$. Along the infinite parts of Γ we use hyperbolic planes as barriers whose asymptotic boundary is tangent to Γ.

Chapter 6

Comparison of Planar Hyperbolic Curves

In this chapter we prove a comparison theorem for planar hyperbolic curves. The result we derive in theorem 37 allows us to estimate the sector angle of a curve γ enclosed by the two geodesics through $\gamma(0)$ and $\gamma(l)$ orthogonal to γ. This is a C^1 estimate on γ. We use information of the turning angle of the normal against a parallel vector field along γ. If the normal vector along γ turns in a certain way faster than the normal vector of a comparison circle, then the sector angle Ψ of γ will be larger than the corresponding and explicitly known sector angle of the circle.

In Euclidean space parallel transport is independent of the chosen path. Therefore the sector angle is identical to the turning angle for every curve. In hyperbolic space the unknown area of the enclosed sector measures the difference between both angles by Gauß-Bonnet (see Polthier [28]).

For infinitesimal short curves we can use the representation formula of the sector angle derived in lemma 32 and estimate the integral-term to get control over the sector angle in terms of the turning angle of the normal vector. For longer curves the integral-term does not seem to be controllable. An additional problem for longer curves is that the comparison statement of the curve's sector angle with a circle's sector angle easily becomes false.

We know about no other comparable result for planar hyperbolic curves, except of Polthier [28], where we applied the representation formula of lemma 32 to short curves. In S^3 Karcher, Pinkall and Sterling [18] used a similar algorithm on discretized turning angle functions for the comparison of spherical planar curves. But our arguments are different from theirs.

The motivation for our study of planar curves originates in the application of the conjugate surface construction method in chapter 8. We will use this method to prove existence of minimal surfaces with higher genus in hyperbolic space. The method makes it necessary to have control about a planar hyperbolic curve γ in terms of the total turning function α of its tangent resp. normal against a parallel vector field along γ. We will discuss the application in chapter 8 in greater detail. Here all arguments are independent of the later application, we only use intrinsic properties of a curve γ about its turning angle function α.

6.1. Properties of Planar Hyperbolic Curves

Let $\gamma : I = [0, l] \to \mathbf{H}^2 \subset \mathbf{R}^3_L$ be a planar hyperbolic curve parameterized by arc length s over the interval $[0, l]$, $l \in \mathbf{R}^+$, with tangent vector t and unit normal n. We denote by (γ', t', n') the derivative of the frame (γ, t, n) in $\mathbf{R}^3_L$ w.r.t. the arc length parameter. Via hyperbolic Frenet theory the curve γ is well-defined up to hyperbolic isometries by its curvature function $\kappa = \kappa(s)$:

$$\begin{pmatrix} \gamma' \\ t' \\ n' \end{pmatrix} = \begin{pmatrix} 0 & 1 & 0 \\ 1 & 0 & \kappa \\ 0 & -\kappa & 1 \end{pmatrix} \begin{pmatrix} \gamma \\ t \\ n \end{pmatrix}. \tag{6.1}$$

Using the technique of Polthier [28], where we transferred a similar method in S^3 of Karcher, Pinkall, Sterling [18] to hyperbolic space, we can reduce the order of differentiability of the determining function. Let a and b be parallel vector fields obtained by parallel translating $t(0)$ and $n(0)$ along γ. Then there exists a function α such that we have along γ:

$$\begin{aligned} a &= t\cos\alpha - n\sin\alpha \\ b &= t\sin\alpha + n\cos\alpha. \end{aligned} \tag{6.2}$$

The function α measures the total turn of the normal n of γ against a parallel vector field generated by parallel translation of $n(0)$. Therefore we define

Definition 30. *The function α is called the* **total turning angle** *of γ.*

The function α also measures the total curvature of γ since

$$\alpha' = \kappa.$$

This can easily be proved by evaluating the right hand side of $\kappa = \langle \gamma'', n \rangle$ in terms of a and b and using the parallelity property.

Using the new frame (γ, a, b) we get another system of differential equations, equivalent to (6.1),

$$\begin{pmatrix} \gamma' \\ a' \\ b' \end{pmatrix} = \begin{pmatrix} 0 & \cos\alpha & \sin\alpha \\ \cos\alpha & 0 & 0 \\ \sin\alpha & 0 & 0 \end{pmatrix} \begin{pmatrix} \gamma \\ a \\ b \end{pmatrix} \tag{6.3}$$

by substituting the expression 6.2.

The new system 6.3 has the advantage that the function α is determined by the derivatives of γ up to order one while we need derivatives up to order two to determine the curvature function κ in system 6.1. This fact is essential when comparing minimal surfaces.

We derive some formulas for a sector of a hyperbolic circle.

Lemma 31. *Consider a sector of a hyperbolic circle in figure 6.1 with curvature $\kappa \in (1,\infty)$, radius r, total turning angle α, enclosed sector angle ψ and length l of the arc. Then we have the following equations:*

$$\begin{array}{rl} \kappa & = \frac{1}{\tanh r} \\ \alpha & = \frac{l}{\tanh r} = l \cdot \kappa = \psi \cdot \cosh r = \frac{\psi \cdot \kappa}{\sqrt{\kappa^2 - 1}} \\ area & = \psi \cdot (\cosh r - 1) \\ \psi & = l \cdot \sqrt{\kappa^2 - 1} = \frac{l}{\sinh r}. \end{array} \tag{6.4}$$

Proof. . is elementary $\left(\text{use } \sinh r = \frac{1}{\sqrt{\kappa^2-1}} \text{ and } \cosh r = \frac{\kappa}{\sqrt{\kappa^2-1}}\right)$.

Lemma 32. *Let γ be a planar hyperbolic curve in $\mathbf{R}^3_L$ parameterized by arc length s with tangent vector t, normal n and total turning angle α with $\alpha(0) = 0$.*

Then the following integral representation exists at length l :

$$\langle t(l), t(0)\rangle = \cos\alpha(l) + \int_0^l \cos(\alpha(l) - \alpha(s)) \langle \gamma(s), t(0)\rangle \, ds \tag{6.5}$$

$$\langle n(l), t(0)\rangle = -\sin\alpha(l) - \int_0^l \sin(\alpha(l) - \alpha(s)) \langle \gamma(s), t(0)\rangle \, ds. \tag{6.6}$$

Proof. . We use the equations 6.2 for the first equality and the system of differential equations 6.3 for the last equality:

$$\begin{array}{rcl} \langle n(l), t(0)\rangle & = & \langle -\sin\alpha(l) \cdot a(l) + \cos\alpha(l) \cdot b(l), t(0)\rangle \\ & = & -\sin\alpha(l) + \langle -\sin\alpha(l) \cdot (a(l) - a(0)) + \cos\alpha(l) \cdot (b(l) - b(0)), t(0)\rangle \\ & = & -\sin\alpha(l) + \left\langle -\sin\alpha(l) \cdot \int_0^l a'(s)ds + \cos\alpha(l) \cdot \int_0^l b'(s)ds, t(0)\right\rangle \\ & = & -\sin\alpha(l) - \int_0^l \sin(\alpha(l) - \alpha(s)) \langle \gamma(s), t(0)\rangle \, ds. \end{array}$$

The proof for equation 6.5 is similar.

6.2. Comparison of Planar Hyperbolic Curves

Let $\alpha_\kappa(s) = s \cdot \kappa$ be the turning angle of a circle γ_κ with constant curvature κ and let $\alpha(s)$ be the turning angle of a planar hyperbolic curve γ. s is arc length parameter defined on the interval $[0, l]$. In this section we give comparison conditions on α and α_κ such that we can estimate the angle ψ enclosed by the two geodesics δ_1, δ_2 through $\gamma(0)$ resp. $\gamma(s)$ with tangent directions $n(0)$ resp. $n(s)$ as in figure 6.2. Since the tangent vector $t(s)$ of γ is for each s normal to the geodesic through $\gamma(s)$ with initial direction $n(s)$ we have

$$\langle t(s), t(0)\rangle = \cos\psi(s) \tag{6.7}$$

in $\mathbf{R}^3_L$ and with lemma 32 the representation

$$\cos\psi(s) = \cos\alpha(s) + \int_0^s \cos(\alpha(s) - \alpha(t)) \langle \gamma(t), t(0)\rangle \, dt. \tag{6.8}$$

Definition 33. *The angle $\psi(s)$ is called the* **sector angle** *of $\gamma_{|[0,s]}$.*

In the following we assume

$$\begin{aligned} \gamma(0) &= \gamma_\kappa(0) \\ t(0) &= t_\kappa(0) \\ n(0) &= n_\kappa(0) \end{aligned}$$

and

$$0 \leq \alpha_\kappa(s) = s \cdot \kappa \leq \alpha(s) \leq \alpha_{\max} \leq \pi \tag{6.9}$$

along the interval $[0, l]$ with $\alpha_{\max} := \max_{s \in I} \alpha(s)$. These inequalities arise from estimating the turning angle of the normal along straight arcs of a minimal surface with a helicoidal comparison surface. The curves γ and γ_κ are well defined by their turning angle functions α and α_κ via equation 6.3. To compare both curves we approximate them by polygons with a small step length h. h is the same for both curves and all steps. The turning angle function of the polygons are step functions over the discrete interval $[0, l]$. They are close to the original functions α and α_κ for small h. We denote the discretized functions also with their original identifiers and then work only with the discretized versions. N is the number of subintervals for a given step length h.

Using the following algorithm we obtain a one parameter family of polygonal curves γ_j which continuously deform γ_κ into γ.

Algorithm:

1. Start with $\alpha_0 := \alpha_\kappa$, $j := 0$
2. Lift the step of α_j over the subinterval $N - j$ to the level of α. Then we have
$$\alpha_j = \{ \begin{array}{l} \alpha \text{ on } [s_{N-j-1}, s_N] \\ \alpha_\kappa \text{ on } [s_0, s_{N-j-1}) \end{array}$$
and the corresponding polygonal curve γ_j equals γ_κ on $[s_0, s_{N-j-1})$.
3. Set $\alpha_{j+1} := \alpha_j$, increment j and continue with 2.

With this algorithm we deform α_κ step by step into α, starting at the end of the interval $[0, l]$. Since all α_j determine via the system 6.3 a curve γ_j and since the system depends continuously on the angle function, the curves γ_j and the functions t_j and n_j deform also continuously. We now derive a sequence of lemmas to control the corresponding sector angles.

To study the effect of step 2 of the algorithm on the corresponding polygon γ_j consider the situation at $\gamma_j(s_{N-j-1})$ and $\gamma_j(s_{N-j})$ in figure 6.4 where $i := N-j-1$.

The effect of step 2 at $\gamma_j(s_i)$ is a rotation $\mathcal{H}$ of $\gamma_{j|[s_i,s_N]}$ with center $\gamma_j(s_i)$ and angle θ_i being the difference of the levels of α minus α_κ over the subinterval (s_i, s_{i+1}). The effect at $\gamma_j(s_{i+1})$ is a rotation $\mathcal{G}$ around $\gamma_j(s_{i+1})$ with angle -θ_i.

So the total effect of step 2 is the identity map on $\gamma_{j|[0,s_i]}$, a rotation of $\gamma_{j|[s_i,s_{i+1}]}$ around $\gamma_j(s_i)$ with angle θ_i and on $\gamma_{j|[s_{i+1},s_N]}$ the product of the two rotations $\mathcal{H} \circ \mathcal{G}$. By lemma 4 this results in a translation T of $\gamma_{j|[s_{i+1},s_N]}$ along a geodesic through $\gamma_j(\frac{s_i+s_{i+1}}{2})$, which encloses with the mid perpendicular of the segment from $\gamma(s_i)$ to $\gamma(s_{i+1})$ an angle $\widetilde{\theta} := \frac{\theta_i}{2} + \epsilon_i$. Using equation 1.5 we have

$$\widetilde{\theta} := \frac{\theta_i}{2} + \epsilon_i = \arctan(\cosh\frac{s_{i+1} - s_i}{2} \cdot \tan\frac{\theta_i}{2}),$$

which is approximately $\frac{\theta_i}{2}$ for small step size h. We consider $\widetilde{\theta}$ and later $\widetilde{\theta}_{crit}$ as step functions on I, therefore we skip their subindex i.

Lemma 34. *Let $\alpha_{\max} \in [0, \pi]$ and α and α_κ fulfilling the condition*

$$0 \leq \alpha_\kappa(s) = s \cdot \kappa \leq \alpha(s) \leq \alpha_{\max} \leq \pi, \ s \in I := [0, l]$$

as in equation 6.9, then each translation direction occurring in step 2 of the algorithm described above intersects the geodesic δ through $\gamma(0)$ with initial direction $n(0)$.

Proof. . The the sector and therefore the interval $I = [0, l]$ have maximal length $l = \pi \tanh r$. This follows from the assumption on $\alpha_{\max}$ and equation 6.4.

Fix j in the algorithm above and set $i := N - j - 1$. Since γ_κ is a circular arc with center M on δ and the axis of translation T encloses an angle $\widetilde{\theta} > 0$ with the geodesic connecting M with $\gamma_\kappa\left(\frac{s_{i+1}+s_i}{2}\right)$, the translation direction can intersect δ at most in a point between M and $\delta(\infty)$.

Let $\widetilde{\theta}_{crit}$ denote the critical value for which T would intersect δ in $\delta(\infty)$ (compare figures 6.4 and 6.5). We show the inequality $\widetilde{\theta}_{crit} > \widetilde{\theta}$ to prove the lemma.

From the geometry of the circle we know that $\widetilde{\theta}_{crit}$ is strictly decreasing from π as ψ resp. s grows. We estimate $\widetilde{\theta}_{crit}$ from below by the angle Ω of the triangle $\Delta_\kappa(M, \gamma_\kappa(0), \gamma_\kappa(\frac{s_{i+1}+s_i}{2}))$ lying inside the triangle $\Delta_\infty(M, \delta(\infty), \gamma_\kappa(\frac{s_{i+1}+s_i}{2}))$ (compare figure 6.5). The two sides of Δ_κ having the vertex M in common are of equal length r. Estimating the area of Δ_κ by the area of the circular sector γ_κ given by equation 6.4 we obtain a lower bound for Ω:

$$\begin{aligned} \Omega &= \tfrac{1}{2}(\pi - \psi - area(\Delta_\kappa)) \\ &> \tfrac{1}{2}(\pi - \psi - area(\text{sector } \gamma_\kappa)) \\ &= \tfrac{1}{2}(\pi - \psi - \psi(\cosh r - 1)) \\ &= \tfrac{\pi}{2} - \tfrac{\psi}{2}\cosh r \end{aligned}$$

For a given curvature κ there exists a positive lower bound ϵ' such that

$$\widetilde{\theta}_{crit} - \Omega > \epsilon' > 0, \text{ for all s} \in I.$$

This follows immediately from the trigonometry of figure 6.5 since γ_κ is always less than a half circle by the assumption. The uniform bound ϵ' is independent of the discretization, it depends only on the curvature κ.

We choose the stepsize h of the discretization small enough such that we have

$$\epsilon_i < \epsilon' \text{ for all i} \in [0, N-1]\,,$$

where $\epsilon_i = \widetilde{\theta} - \frac{\theta_i}{2}$ is defined above.

We are now in a position to estimate $\widetilde{\theta}_{crit} > \widetilde{\theta}$ at an arbitrary node of the step function γ_κ:

$$\begin{aligned}
\widetilde{\theta}_{crit} - \widetilde{\theta} &= \widetilde{\theta}_{crit} - \tfrac{\theta_i}{2} - \epsilon_i \\
&> \Omega + \epsilon' - \tfrac{\theta_i}{2} - \epsilon' \\
&= \Omega - \tfrac{\alpha(s_i) - \alpha_\kappa(s_i)}{2} \\
&\geq \Omega - \tfrac{\alpha_{max}}{2} + \tfrac{\alpha_\kappa(s_i)}{2} \\
&\geq \Omega - \tfrac{\pi}{2} + \tfrac{\psi \cosh r}{2} \\
&> 0
\end{aligned}$$

The first inequality uses the lower bound for $\widetilde{\theta}_{crit}$ and the upper bound on ϵ_i derived above. In the second inequality we use the upper bound π for α from the assumption, and substitute $\alpha_\kappa(s_i)$ in the third inequality by its explicit formula from equation 6.4. The final inequality uses the estimate on Ω.

The following lemmas will be used when studying the effect of a translation occurring in the lift of α_κ to α.

Lemma 35. *Let δ be a geodesic through the point $\mathcal{O}$ together with the family of all perpendicular geodesics to δ. Further, let T be an axis of translation from A to C through $\mathcal{O}$ together with the family of all orbits of T. Let σ_1 and σ_2 be two orbits of T, $\delta^\perp$ be the geodesic perpendicular to δ in $\mathcal{O}$ intersecting σ_1 and σ_2 in B and D as in figure 6.6.*

Then the angle between the orbit σ_1 and the perpendicular geodesics to δ

1.) monotonically decreases from A to B

2.) monotonically increases from B to C

and the angles between the orbit σ_2 and the perpendicular geodesics to δ

3.) monotonically decreases from A to D

4.) monotonically increases from D to C.

Proof. . The problem is symmetric w.r.t. σ_1 and σ_2 and we restrict to proving the assumption for σ_1.

a) The shown angle between T and the perpendicular geodesics is decreasing from $\mathcal{O}$ to A and from $\mathcal{O}$ to C. This follows immediately from hyperbolic trigonometry applyed to triangles enclosed by δ, T and the δ-perpendiculars.

b) If we parallel translate the geodesic segment $\mathcal{O}B$ along T to the segment $T(\mathcal{O}B)$ with new end points $T(\mathcal{O})$ and $T(B)$ then the angles at $T(\mathcal{O})$ and $T(B)$ will remain constant.

c) From a) and b) it follows that the δ-perpendicular through $T(\mathcal{O})$ crosses the triangle $(A, T(\mathcal{O}), T(B))$. Therefore the δ-perpendicular through $T(B)$ crosses the quadrilateral $(T(B), T(\mathcal{O}), \mathcal{O}, B)$, and its shown angle at $T(B)$ with the orbit curve is bigger than the angle at B.

d) Since the angle in a) is monotonicly decreasing from $\mathcal{O}$ to A we could use any other δ-perpendicular as initial geodesic segment for the comparison argument in b) and c).

This proves 1.

To prove 2. we use a corresponding argument as in b) and c) with translation along T in direction of C.

Lemma 36. *Let δ be a geodesic with its family of distant curves. Let T be a geodesic insecting δ. Then every distance curve σ of T intersects each distance curve of δ exactly once (compare figure 6.7).*

Proof. . The distance curves to T resp. δ are the orbits of a hyperbolic translation along T resp. δ. They are segments of hyperbolic circles with constant curvature $\kappa \in [0, 1)$ through $T(-\infty)$ and $T(+\infty)$ resp. $\delta(-\infty)$ and $\delta(+\infty)$. Let σ be an orbit of T. Then every orbit of δ intersects σ at least once since σ separates $\delta(-\infty)$ and $\delta(+\infty)$. Suppose σ intersects an orbit of δ more than once. This means it intersects exactly twice since both orbits have constant curvature. Then both ends of the orbit of δ lie on one side of σ contrary to the above separating property of σ.

We are now in a position to prove the main comparison theorem for a planar hyperbolic curve γ. This is a C^1 estimate comparing the tangent vectors at $\gamma(0)$ and $\gamma(l)$ with each other using knowledge only about the total turning function α of the tangent resp. normal vector along γ. Despite the technical restrictions we have to make on the situation it turns out that more general conditions easily make the statements false. This contrasts very much to the Euclidean case, where the sector angle of a curve is identical to the turning angle. Compare also the helicoidal comparison theorem in $\mathbf{R}^3$ of Karcher [16].

Theorem 37 [Comparison of Planar Curves]**.** *Let γ be a planar hyperbolic curve and γ_κ a sector of a hyperbolic circle with constant curvature $\kappa \in (1, \infty)$, both defined over an interval $[0, l]$ and parametrized by arc length s. Further, let α resp. α_κ be the turning angle functions of γ resp. γ_κ fulfilling the condition*

$$\forall s \in [0, l] : \; 0 \leq \alpha_\kappa(s) = s \cdot \kappa \leq \alpha(s) \leq \alpha(l) \leq \pi,$$

and the sector angle ψ_κ of the circle satisfies

$$\psi_\kappa \geq \frac{\pi}{2}.$$

Then the sector angle ψ of γ is larger than the sector angle ψ_κ of the circle, i.e. we have:

$$\psi \geq \psi_\kappa = l \cdot \sqrt{\kappa^2 - 1} \geq \frac{\pi}{2}.$$

For a given curvature κ, the inequalities $\alpha_\kappa(l) \leq \pi$ and $\psi_\kappa \geq \frac{\pi}{2}$ are equivalent to restrictions on the length l of the curves:

$$\frac{\pi}{2\sqrt{\kappa^2 - 1}} \leq l \leq \frac{\pi}{\kappa},$$

and they are also equivalent to restrictions on α_κ:

$$\frac{\pi\kappa}{2\sqrt{\kappa^2 - 1}} \leq \alpha_\kappa(l) \leq \pi.$$

Proof. . We will apply our lifting algorithm to deform γ_κ to γ and prove that the corresponding sector angles monotonically increase during each step. In the following we denote with $G(p, q)$, $p \in H^2$ and $q \in T_pH^2$, a geodesic through p with initial direction q.

We assume that α and α_κ are given as step functions on a discretization $0{=}s_0 < s_1 < ... < s_N = l$ with a suitable small step length. Using our lifting algorithm we construct a family of step functions

$$\{\alpha_j\}_{j\in\{0,..,N-1\}}$$

deforming γ_κ into γ. Let $i = N - j - 1$ and consider the effect of the lift α_j to α_{j+1} on the change ψ_j to ψ_{j+1} of the corresponding sector angles. As discussed before the total effect of the lift is

- the identity on $\gamma_{j|[0,s_i]}$
- a rotation on $\gamma_{j|[s_i,s_{i+1}]}$ around $\gamma_j(s_i)$ with angle $\theta_i = \alpha(s_i) - \alpha_\kappa(s_i)$
- a translation on $\gamma_{j|[s_{i+1},s_N]}$ along an axis T_i.

Therefore the change ψ_j to ψ_{j+1} is the effect of the translation T. Because of lemma 34 T intersects the geodesic $\delta = G(\gamma_j(0), n_j(0))$. The geodesic $G(\gamma_j(l), -n_j(l))$ is parallel translated by T to the geodesic $G(\gamma_{j+1}(l), -n_{j+1}(l))$. Since T intersects δ we can apply lemma 35 to prove that the angle of $G(\gamma_j(l), -n_j(l))$ and the geodesic $\delta^\perp(\gamma_j(l)$ through $\gamma_j(l)$ and perpendicular to δ is increasing under the translation T:

If T intersects δ in direction of $\delta(\infty)$ then $\gamma_j(l)$ is on an orbit of T between points A and D, compare figure 6.6. During translation the angle of $G(\gamma_j(l), -n_j(l))$ with the orbit of $\gamma_j(l)$ is constant and therefore we can use lemma 35 to see that the angle ϕ of $G(\gamma_j(l), -n_j(l))$ with the $\delta-$perpendicular, as indicated in figure 6.6, is increasing.

If T intersects δ in direction of $\delta(-\infty)$ then $\gamma_j(l)$ is on an orbit of T between points B and C, because of the assumption in the theorem $\psi_\kappa \geq \frac{\pi}{2}$ and further translations increase the angle. Since the angle of $G(\gamma_j(l), -n_j(l))$ with the orbit of $\gamma_j(l)$ is constant we use lemma 35 in the same way as above to prove that the indicated angle of $G(\gamma_j(l), -n_j(l))$ with the $\delta-$perpendicular is increasing.

Therefore, during the lift from α_j to α we increase in each single step the angle of $G(\gamma_j(l), -n_j(l))$ with the $\delta-$perpendiculars. Since $G(\gamma_j(0), n_j(0)) = \delta$ the sequence of sector angles $\{\psi_j\}$ between δ and $G(\gamma_j(l), -n_j(l))$ is monotonically increasing from ψ_κ to ψ.

This proves the theorem.

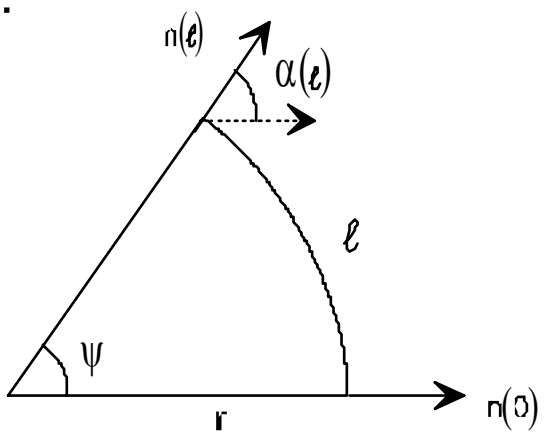

Figure 6.1: Sector of a Circle

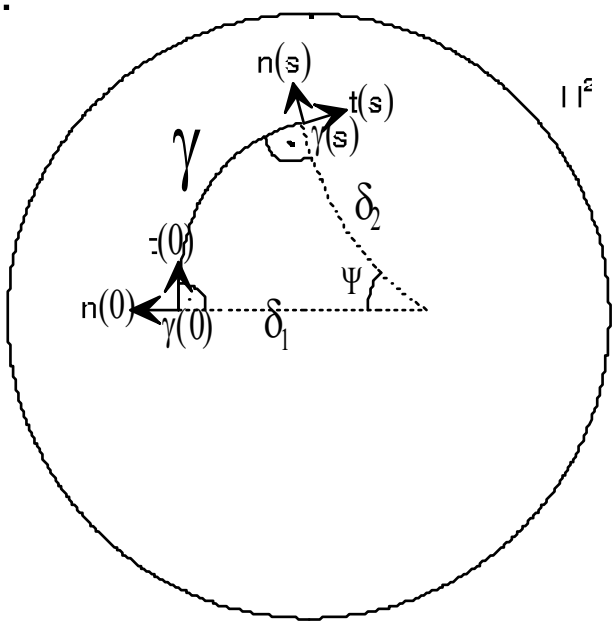

Figure 6.2: Notation for a Planar Curve

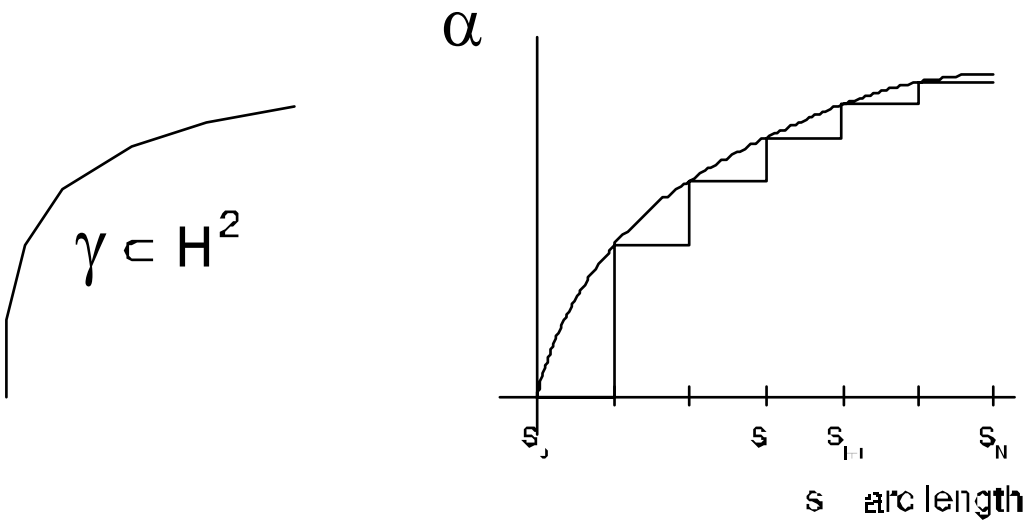

Figure 6.3: Turning Angle as Step Function

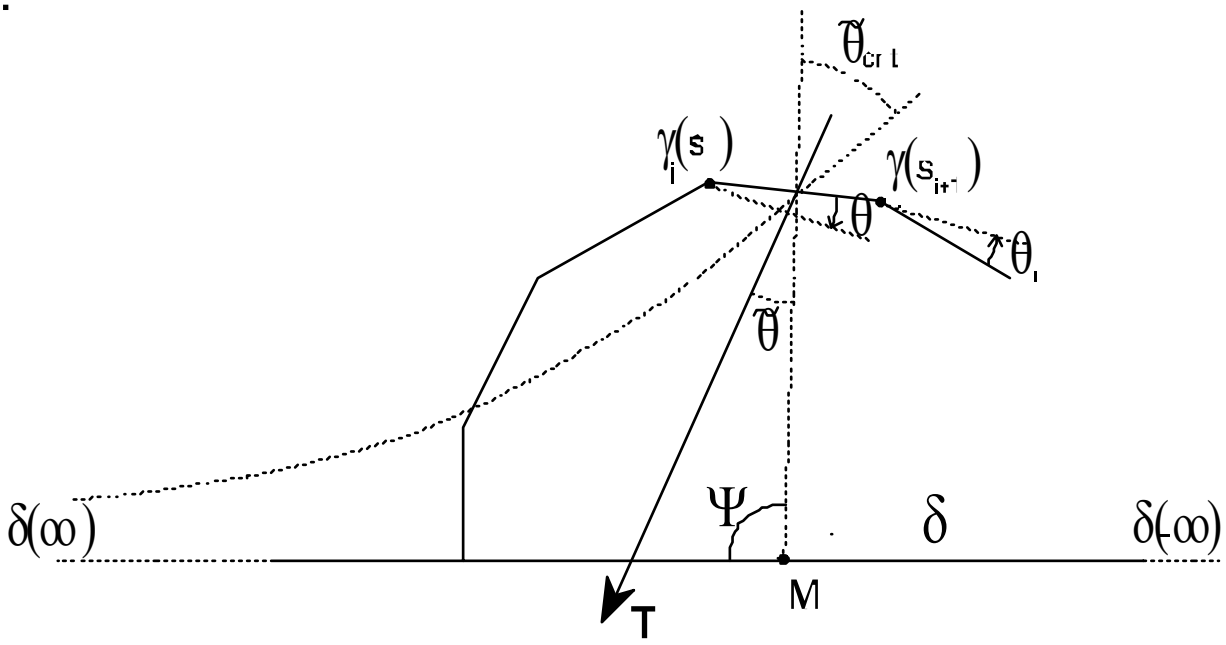

Figure 6.4: The Effect of a Single Step of the Deformation Algorithm

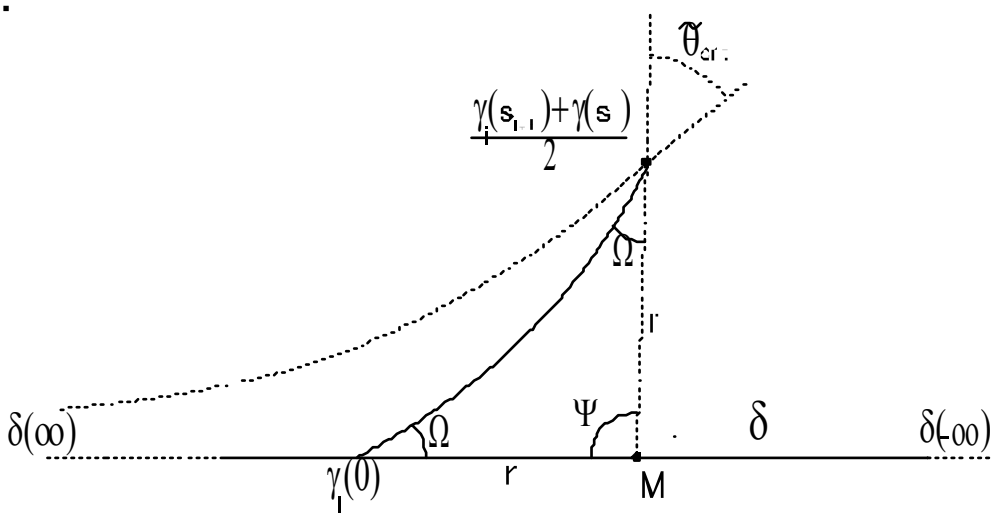

Figure 6.5: Estimate of the Critical Angle

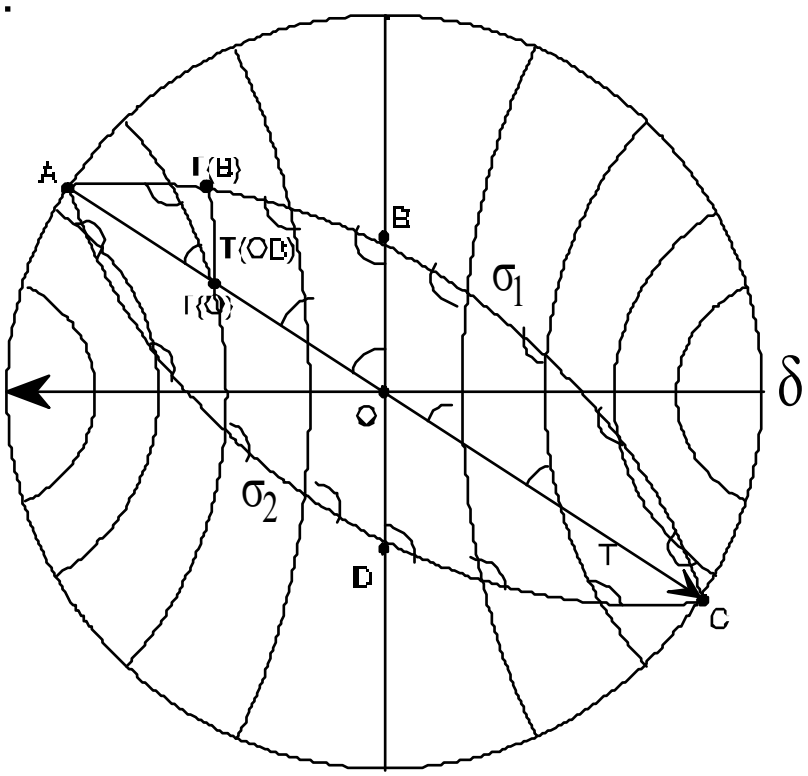

Figure 6.6: Angles along Translation

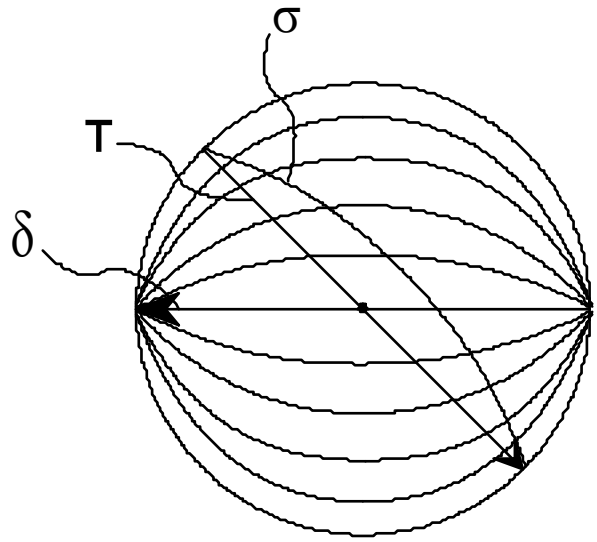

Figure 6.7: Levels along Translation

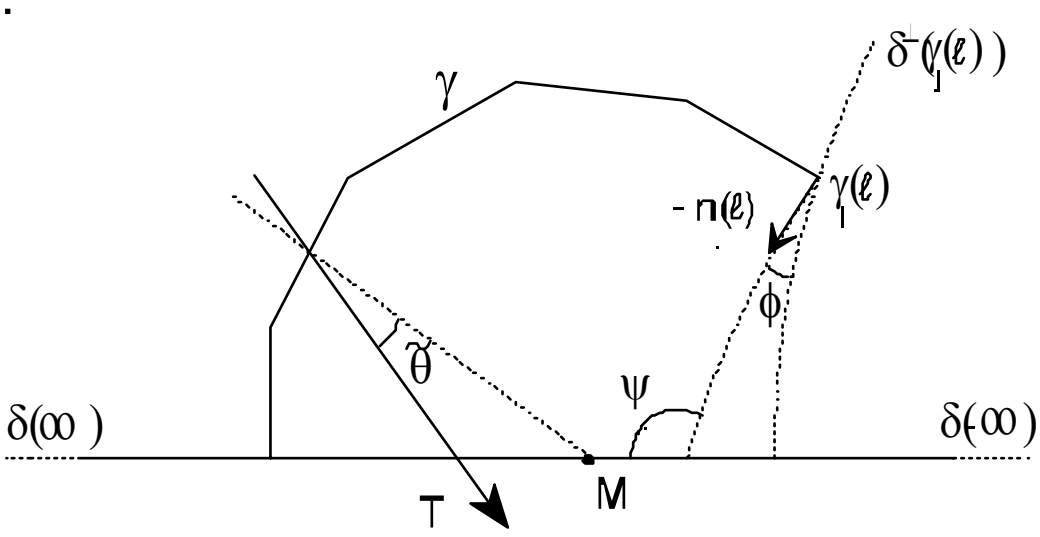

Figure 6.8: Change of Sector Angle

Chapter 7

Direct Examples

This section is intended to be an application of chapter 5. We discuss a number of new complete embedded examples of periodic minimal surfaces in H^3. We prove existence of a fundamental piece by using theorem 29 of chapter 5. The term "direct" in the title indicates that we explicitly supply boundary contours. In our examples the finite part consists in each case of a number of polygonal arcs, i.e. segments of hyperbolic geodesics. All fundamental pieces discussed below extend by successive $180°-$reflection around finite polygonal arcs to complete embedded minimal surfaces in H^3. In contrast to the Euclidean case we have much more freedom in choosing the part of the contour lying on S^∞. As long as the projection property for theorem 29 is fulfilled, we may vary the infinite part. Compare this to the theorem of Jenkins and Serrin 27 where it is proved that the infinite part is asymptotic to a Euclidean plane.

Some of our examples have contours similar to those of classical minimal surfaces in Euclidean space. We call these surfaces "hyperbolic cousins". This term was introduced by R. Bryant in his study of hyperbolic $H \equiv 1$ surfaces which are isometric to Euclidean minimal surfaces.

The first example is discussed in greater detail to illustrate the application of theorem 29. In the discussions we usually do not always mention the possibility of modifying the infinite part of the boundary. For a clearer presentation we have chosen this part to be asymptotic to a hyperbolic plane usually.

7.1. Hyperbolic First Scherk Cousins

This example is similar to the Euclidean 1. Scherk surface and its generalizations. The building block for the translational symmetry group of the Euclidean 1. Scherk surface is a Jenkins/Serrin graph over a black field of a chess board with values $+\infty$ along the horizontal and $-\infty$ along the vertical sides of the field (compare theorem 27). Two further straight lines on the building block crossing at the saddle point (the two diagonals of the field) divide it into four congruent pieces. The complete surface is obtained by successively reflecting the block at its vertical straight lines over the vertices of all black fields. This surface is then a graph over all black fields of the chess board.

In hyperbolic space we can simulate this procedure. To setup the correspond-

ing Jenkins/Serrin problem, we look for a tessellation of H^2 by regular hyperbolic quadrilaterals and a dual regular n-gon such that inversion at the vertices of the quadrilaterals maps each quadrilateral exactly into another quadrilateral, i.e. the inversion induces an isometry of the tessellation. Additionally we need that edges with initial values $+\infty$ resp. $-\infty$ are mapped to edges with $+\infty$ resp. $-\infty$. Consider the tessellation of figure 7.1.

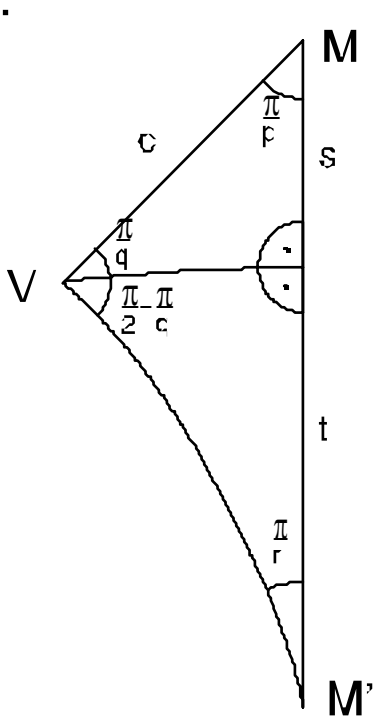

The two fundamental triangles are drawn in a separate figure. The condition

$$p, r \equiv 0 (mod\ 2)$$

is necessary and sufficient for the existence of a tessellation of H^2 with regular p-gons and r-gons such that edges with $+\infty$ resp. $-\infty$ always correspond to edges with $+\infty$ resp. $-\infty$. In this cases $q \in \mathbf{R}$ is determined by the choice of p and r by

$$\tan\frac{\pi}{q} = \frac{\cos\frac{\pi}{p}}{\cos\frac{\pi}{r}}.$$

$r = \infty$ denotes the case when $\frac{\pi}{r}$ degenerates to 0. In this case all vertices of the dual polygon lie on a horocircle with center $M' \in S^\infty$.

For a given p we can now increase q further but the dual polygon will no longer close since M' is beyond S^∞. From now on the complete minimal surface will be simply connected. The flexibility of this situation stays in marked contrast to

minimal surfaces in Euclidean space. It gives a feel for the huge amount of space available in hyperbolic space.

We can increase q further to ∞. In this limit case the whole tessellation consists of exactly one ideal quadrilateral with a non periodic embedded complete minimal surface inside.

To prove that the tessellation is correct everywhere, i.e. no gaps or overlaps occur, it is sufficient to check this around the two neighboring fundamental polygons. Then the global correctness follows in a similar way by a Poincaré argument as in the case of tessellating H^2 with congruent triangles.

Now we prove existence of a fundamental minimal patch for a fundamental triangle of an arbitrary tessellation as discussed above. Consider the hyperbolic Jenkins/Serrin contour for the First Scherk Cousin in figure 7.2.

We choose the projection center $p_0 \in S^\infty$ to lie somewhere above the shaded region close to vertex M. The infinite part of the contour may for example be asymptotic to the hyperbolic plane being orthogonal to the triangle along the geodesic through V_1 and V_2. But it may be different from that as long as still a projection center p_0 with the required property exists. Then the contour p-projects onto a p-convex curve on S^∞ for all $p \in B$, $B \subset S^\infty$ a small neighbourhood of p_0. In figures 7.3 and 7.4 we show a piece of a First Scherk Cousin with $p = 4$ and $r = 6$ and the complete surface.

In figure 7.6 we show a non-periodic First Scherk Cousin. This surface is the limit case, when in the points V_1 and V_2 in the Jenkins/Serrin contour become ideal points on S^∞, i.e. $q = \infty$.

7.2. Variation of the First Scherk Cousin

A variation of the hyperbolic Scherk surface works only partially. Consider the Jenkins/Serrin graph in figure 7.5 consisting of two isometric fundamental pieces. When reflecting the minimal surface around the vertex V_1 we obtain q $\infty-$half planes and q (-∞)-half planes intersecting at the vertical geodesic at V_1. Therefore the surface would not be embedded. If we choose $q = \infty$, V_1 becomes an ideal point and the half planes no longer intersect. The problem is still well-defined and we obtain a complete minimal surface which can be described as follows: Take a hyperbolic plane and tessellate it with regular ideal p-gons. Along the edges of all p-gons intersect the plane orthogonally with vertical planes. Replace the singular intersection lines by two holes.

7.3. Hyperbolic Second Scherk Cousin

The hyperbolic pendent of the second Scherk surface, the simply periodic Scherk tower, can be directly constructed or constructed via the conjugate surface method

(compare chapter 8). For the direct construction we choose a hyperbolic Jenkins/Serrin contour with two ends similar to that in figure 7.8. The only difference is, that two boundary geodesics joining the same end must belong to the same hyperbolic plane, i.e. both geodesic pairs are not twisted against each other.

The projection center p_0 lies on S^∞ between the two planes spanned by the two pairs of boundary geodesics to assure the required projection property of theorem 29. The angle at the two finite vertices is $\frac{\pi}{k}$, $k \in \mathbf{N}$, and k determines the order of the saddle point. Compare figure 7.7 for a picture of the complete surface. As in the Euclidean case the saddle tower looks, from a distance, as k planes intersecting in a single line. Moving closer, this line is replaced by a system of alternating holes. A further parameter of the construction is the hyperbolic distance of the two finite vertices in the initial contour. As in the Euclidean case one may cut the infinite parts of the contour at finite distance along hyperbolic geodesics and obtain a family of triply periodic surfaces. But this construction needs further restrictions, since the new geodesics have to intersect the original boundary at natural angles, i.e. angles of the form $\frac{\pi}{l}, l \in \mathbf{N}$.

7.4. Hyperbolic Helicoidal Saddle Towers

Helicoidal hyperbolic saddle towers corresponding to Karcher's construction in $\mathbf{R}^3$ [14] may be obtained by rotating the two geodesic boundary arcs at M around the geodesic from M to M' by an arbitrary angle in figure 7.8. The geodesic boundary arcs intersect the geodesic from M to M' orthogonally. The complete embedded helicoidal saddle tower is shown in figure 7.9.

Figure 7.1: Tesselation of H^2 by Regular Quadrilaterals

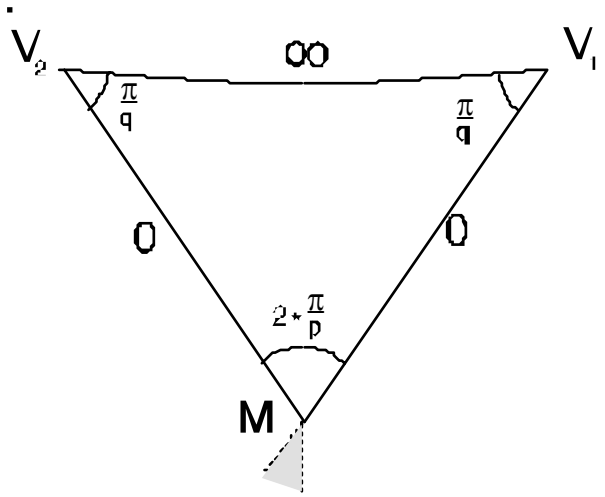

Figure 7.2: Contour for Hyperbolic First Scherk Cousin

Figure 7.3: Fundamental Piece of First Scherk Cousin with Tessellation

Figure 7.4: Complete First Scherk Cousin (p=4, r=6)

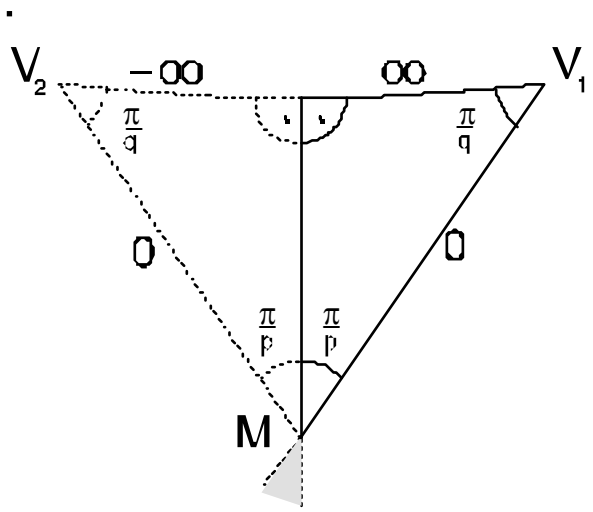

Figure 7.5: Variation of Scherk's First Surface

Figure 7.6: Non Periodic Example of the First Scherk Cousin

Figure 7.7: Second Scherk Cousin (k=2)

Figure 7.8: Fundamental Contour for Hyperbolic Helicoidal Saddle Tower

Figure 7.9: Hyperbolic Helicoidal Saddle Tower

Chapter 8

Examples via Conjugate Surface Construction

8.1. The Conjugate Surface Construction

The conjugate surface construction method is a powerful tool for proving existence of minimal surfaces whose finite boundary parts consist of planar lines of symmetry. In general, these surfaces are instable such that minimization arguments are often not available. Lawson [19] used this method first to prove existence of Euclidean $H \equiv 1$ surfaces via a conjugate surface construction in S^3. In [34] Smyth used this construction to prove existence of three minimal patches in each Euclidean tetrahedron. Karcher, Pinkall, Sterling [18] resp. Polthier [29] applied the conjugate surface method to minimal surfaces in S^3 resp. H^3. Compare also Karcher's work in [15] and [16] who refined the arguments controlling the method in $\mathbf{R}^3$ and used it in many existence proofs.

We now give a short introduction into this method. Assume a free boundary value problem for a minimal surface, i.e. parts of the boundary are restricted to planes and the surface shall intersect this planes orthogonally. Instead of solving this problem directly we can try to construct the conjugate minimal surface. By the results of section 2.2 this is an equivalent formulation of the problem. In the case mentioned above the conjugate contour would consist of polygonal boundary arcs. The angles of the polygon are known from the free boundary value problem, since both surfaces would be isometric. In some cases in $\mathbf{R}^3$ this is enough information to determine the conjugate contour exactly. Solving the Plateau problem for the polygonal contour and conjugating the surface would lead to a solution of the initial problem.

The biggest problem is usually, that the conjugate polygonal contour is not uniquely determined. Therefore, being able to estimate the planar arc corresponding to a straight arc is a necessary condition to apply the conjugate surface construction.

We derive such estimates in our following theorem 38 based on the results of chapter 6. In the following, this theorem will be our working horse to control the hyperbolic conjugate surface construction. We use the theorem to show that the two normal geodesics at the end points of a planar arc are orthogonal, i.e. $\psi = \frac{\pi}{2}$.

Consider a standard situation in the conjugate surface construction as in figure 8.1.

Theorem 38 [Comparison with Helicoid]**.** *Assume a situation in the conjugate surface construction as in figure 8.1. A minimal surface M contains a straight arc γ of length $l \leq \frac{\sqrt{3}\pi}{2}$ and has a helicoid as a barrier surface from below with axis γ, i.e. the two turning angle functions α and α_κ satisfy*

$$\alpha_\kappa(0) = \alpha(0) = 0$$
$$\alpha_\kappa(s) \leq \alpha(s) \leq \alpha(l) \leq \pi,\ s \in [0,l]$$

and

$$\sqrt{\frac{\pi^2}{4} + l^2} \leq \alpha_\kappa(l) = \alpha(l).$$

If further there exists a one parameter deformation M_t, $t \in [0,1]$ of $M =: M_0$ such that the corresponding functions α_t and l_t vary continuously and

$$\alpha_1(l_1) < \frac{\pi}{k}$$

then there exists a surface M_{t_0}, $t_0 \in [0,1]$, such that the sector angle ψ_{t_0} of the conjugate surface $M^*_{t_0}$ fulfills

$$\psi_{t_0} = \frac{\pi}{k}.$$

1.) The condition $l \leq \frac{\sqrt{3}\pi}{2}$ is no additional restriction, it only assures that $\sqrt{\frac{\pi^2}{4} + l^2} \leq \alpha(l) \leq \pi$ can be fulfilled. In standard applications of this lemma it is often possible to choose $\alpha(l) = \pi$. Choosing $l \leq \frac{\sqrt{3}\pi}{2}$ in such cases will generally satisfy all necessary conditions of the lemma.

2.) The continuous dependence of α_t on t will be shown in each application separately by using different barrier surfaces adapted to the specific situation.

3.) Instead of $\psi_{t_0} = \frac{\pi}{k}$ the proof shows that every angle less or equal $\frac{\pi}{2}$ may occur.

Proof. . We will apply theorem 37 to prove that the sector angle ψ_0 of $M_0 = M$ is larger than $\frac{\pi}{2}$. The assumed inequalities for $\alpha(s)$ are the required condition on α for the theorem. From lemma 31 we have

$$\kappa = \frac{\alpha_\kappa(l)}{l}$$

and

$$\psi_\kappa = l\sqrt{\frac{\alpha_\kappa(l)^2}{l^2} - 1} = \sqrt{\alpha_\kappa(l)^2 - l^2}.$$

Using the inequality $\sqrt{\frac{\pi^2}{4}+l^2} \leq \alpha(l) = \alpha_\kappa(l)$ we can estimate ψ_κ :

$$\psi_\kappa \geq \sqrt{\frac{\pi^2}{4}+l^2-l^2} \geq \frac{\pi}{2}.$$

Therefore we can apply theorem 37 and deduce that

$$\psi_0 \geq \frac{\pi}{2}$$

for the sector angle ψ_0 of the conjugate arc γ_0^*.

For M_1 we have $\alpha_1(l_1) < \frac{\pi}{k}$ and $\psi_1 < \alpha_1(l_1)$. By the assumption α_t, l_t vary continuously w.r.t. t. The same is true for the sector angle ψ_t since the system of differential equations 6.3 depends continuously on α_t and l_t. Therefore the intermediate value theorem on ψ_t proves existence of a value $t_0 \in (0,1)$ such that

$$\psi_{t_0} = \frac{\pi}{k}.$$

8.2. Again, Hyperbolic Second Scherk Cousin

We start these examples with the hyperbolic version of the Euclidean Scherk tower, also known as Scherk's second surface. The most symmetric version was already discussed in chapter 7 when we used the fact that this surface is divided into simply connected pieces by the straight lines lying on it. We prove existence of this surface again via the conjugate surface construction, demonstrate the application of our helicoidal comparison theorem 38 for the first time and thereby obtain also deformations of the symmetric Scherk surface which contain no longer straight lines, i.e. they do not appear as Morrey solutions of a direct construction.

Consider the contour in figure 8.2 and assume for the moment $l = l'$, i.e. a symmetric contour. We can solve the corresponding Plateau problem using our existence theorem 29. Let M be the minimal surface in this contour. We use our helicoidal comparison theorem to prove existence of a value $\alpha_0 \in \left[\frac{\pi}{2}, \pi\right)$ such that the conjugate arcs of AB and DB have sector angles $\frac{\pi}{2}$.

We choose a helicoid as a barrier with axis A and B, and having the same tangent planes in A and B as M. For a given length l of the arc AB with $l \leq \frac{\sqrt{3}\pi}{2}$ we choose $\alpha(l) \in \left[\sqrt{\frac{\pi^2}{4}+l^2}, \pi\right)$. Now all conditions of theorem 38 are fulfilled, it remains to prove continuous dependence of the turning angle function on variations of the contour: if we fix l and reduce $\alpha(l)$ by ϵ we obtain a minimal surface $\widetilde{M}$. M is a barrier to $\widetilde{M}$ along the arc AB from the outside. To get a barrier from the inside we translate M along AB in direction of A so far that the barrier helicoid of M along AB separates the arc $\widetilde{A}\widetilde{C}$ from the translate of M. Then we know that the translate of M is a barrier from inside since it leaves the

contour of $\widetilde{M}$ on one side. The shift of M is of the same order as ϵ and $\widetilde{M}$ has to lie between M and its translated copy. Therefore we have

$$\forall s \in [0, l] \colon \widetilde{\alpha}(s) - \alpha(s) < \wr(\epsilon).$$

The same arguments work simultaneously along the arc DB. This proves existence of the hyperbolic Scherk tower via conjugate surface construction.

8.3. Non-Symmetric Scherk Tower

The arguments for the symmetric tower for both arcs AB and DB are independent of each other. For given l and $l^{'}$ with l ¿ $l^{'}$ we can argue on both arcs as above and obtain by an intermediate value argument that there exists a surface such that the two sector angles ψ and $\widetilde{\psi}$ on the conjugate arcs are rectangular. Since $l \neq l^{'}$ the surface M has lost its reflectional symmetry. On the conjugate surface M^* we therefore have no longer straight lines.

8.4. First Scherk Cousin With Handle

This modification of the first Scherk surface was first done by Karcher [14] in Euclidean space. The saddle of a fundamental piece is replaced by a handle. The complete surface has the same translational symmetry group as the original 1. Scherk surface.

To prove existence in hyperbolic space we have a closer look at the conjugate contour in figure 8.3. The sector angle along the edge l_1^* has to be made $\frac{\pi}{2}$. Therefore, depending on the length l_1, we choose the total turning angle $\alpha(l_1)$ of the normal along AB to lie in the interval $\left[\sqrt{\frac{\pi^2}{4} + l_1^2}, \pi\right)$ to apply lemma 38. The same barrier arguments as for the singly periodic Scherk tower ensure the continuous dependence of the change of the normal along AB w.r.t. variations of $\alpha(l_1)$.

This proves the existence of a hyperbolic Scherk handle above an equiangular quadrilateral. Further estimates on the curves l_1^* and l_2^* would be necessary to assure existence of a surface of this type also above an equiangular quadrilateral with all sides of equal length (see figures 8.4 and 8.5).

8.5. Hyperbolic $k-$noid Cousins

The hyperbolic k-noids are surfaces with a multiple number of horizontal catenoidal ends as their Euclidean pendants of Jorge and Meeks [13]. For $k = 2$ we have a rotational symmetric hyperbolic catenoid with two ends. This surface comes with an explicit parameterization since the differential equation for the meridian can be integrated [4]. The catenoid comes in a one-parameter family of surfaces where the curvature κ of the circular waist varies in $(0, \infty)$. For $\kappa \leq 1$ the catenoids are

simply connected and do no longer have an axis of rotation. We will recognize the same behavior on the $k-$noids too.

Consider the conjugate contour for a hyperbolic $k-$noid in figure 8.6. The sector angle β^* has to be rectangular. For this we must control the turning angle α along the arc AB on the conjugate contour. As in the construction of the second Scherk cousin we use a helicoid with axis AB and tangent to the contour in A and B to have a circular comparison curve for theorem 38. For a given length l we choose $\alpha(l) \in \left[\sqrt{\frac{\pi^2}{4}+l^2}, \pi\right)$ to fulfill all estimates of the lemma. The continuity arguments are similar to the argumentation of the second Scherk surface, but depend here on the choice of the part of the boundary lying on S^∞ during rotation of $\alpha(l)$. For the second Scherk surface the asymptotic boundary was always part of the limit of the same hyperbolic plane. The arguments here depend also on the fact whether the plane orthogonal to AB in A intersects the line BD. This is the case for small l, while for larger l and small q they do not intersect. Let us assume they do not intersect. We choose as an asymptotic boundary from C to D a segment of a circle on S^∞ such that for larger $\alpha(l)$ the same construction gives a curve on S^∞ lying in the halfspace which is bounded by the plane ACD and which contains B. Also changing $\alpha(l)$ by ϵ the asymptotic circular arcs shall change only $\wr(\epsilon)$ w.r.t. the Euclidean metric. Then we can argue as for the second Scherk surface: When reducing $\alpha(l)$, the original surface is a barrier for the turning angle α along A to B from above. For an estimate from below we translate the original surface in the direction of A a small amount until it leaves the edge AC on one side. This is assured by using a helicoidal barrier as in the barrier construction for the second Scherk surface. Therefore we can apply theorem 38 to prove existence of a sector angle $\beta^* = \frac{\pi}{2}$. The argument was independent of k and we obtain the whole family of hyperbolic $k-$noids.

If the plane orthogonal to AB in A intersects the line BD we choose the asymptotic circular arcs in such a way that for larger $\alpha(l)$ they lie in the halfspace which does not contain B and reverse the roles of the barrier surfaces in the arguments.

Compare figure 8.7 for hyperbolic trinoids. The size of the ends was modified in the family.

Similar to the situation of the hyperbolic catenoids with waist curvature $\kappa \leq 1$, we can make the sector angle β^* of the k-noid vanish. Even more, we can produce a situation such that the two normal geodesics at A^* and B^* have positive distance. This can be controlled by making the total turning angle $\beta = \alpha(l)$ of the conjugate contour small enough, l large enough. This again contrasts very much to the situation in Euclidean space.

8.6. Platonoids: From Triply Periodic to Non Periodic

In Polthier [29] I proved existence of minimal surfaces in all regular hyperbolic polyhedra and in a large class of Coxeter orthoschemes (compare theorem 26). The fundamental cells of some of these minimal surfaces sit in the same way in polyhedra as the Euclidean Schwarz surface in a cube with handles to all faces (compare figure 8.8). Existence of these surfaces was proved using a conjugate surface construction and solving a two parameter problem. The possible conjugate quadrilateral contours come in a two parameter family.

Now we try to increase the almost circular curves of all polyhedral faces and move to infinity to produce catenoidal ends. The resulting surface will look similar to the k-noids of Jorge and Meeks [13] with additional catenoidal ends. For the existence proof of the platonoids consider figure 8.9. The conjugate contour is similar to the conjugate contour of the k-noids. The difference is, that the relevant sector angle β^* on the surface has to be $\frac{\pi}{2}$ for k-noids. For $(p,q)-$platonoids it must be a specific value $\beta_0^*{=}\beta_0^*(p,q) < \frac{\pi}{2}$ depending on p and q. The exact value of β_0^* is not of interest here. It may be computed for the pyramid with peak M and three dihedral angles $\frac{\pi}{p}$, $\frac{\pi}{q}$ and $\frac{\pi}{2}$ by intersecting the pyramid with a unit sphere with center M. Then one can easily compute β_0^* by spherical trigonometry.

To control β^* we use theorem 38 and choose as in the case of the k-noids a contour such that $\beta^* > \frac{\pi}{2}$ and another contour with $\beta < \beta_0^*$ such that $\beta^* < \beta_0^*$. The continuity arguments are the same as those for k-noids. This proves existence of a fundamental piece for a platonoid with the symmetry of each of the five platonic solids.

We can now extend the idea of moving circular arcs to infinity to other triply periodic candidates. The above platonoids originated in surfaces with a Schwarz handle through each face of the platonic solid. For the Euclidean cube, E.R. Neovius proved existence of a triply periodic surface whose cell has handles to all edges of the cube. We proved in Polthier [29] that such surfaces also exist in some hyperbolic platonic solids. A. Schoen constructed another cell in a cube with handles to all eight vertices, the $I-WP$ surface. The $I-WP$ idea does not lead to new minimal surfaces in hyperbolic space: when the handles are extended to infinity we obtain only a surface which is identical to a Schwarz type platonoid in the dual polyhedron. For example, extending the handles of the $I-WP$ type surface in a hyperbolic cube to infinity leads to the same surface when extending the Schwarz type handles of a cell in a hyperbolic octahedron to infinity.

We do not discuss the Platonoids of Neovius type here, because the arguments depend on odd angles of the Coxeter orthoscheme. The choice of the projection center, the asymptotic curve, the length of the side AB and the continuity arguments would all need special considerations.

8.7. Catenoid with Handles

In Euclidean space Hoffman and Karcher constructed what they called a fence of catenoids. A building block for this translational symmetric surface is topologically a catenoid with two horizontal handles, emanating at opposite points of the waist. By successive reflection at the vertical symmetry planes of the handles the complete fence of catenoids is generated. By increasing the number of handles around a waist one can increase the symmetry.

We now consider such surfaces in hyperbolic space. The conjugate contour of these candidates is similar to the contour of the hyperbolic first Scherk surface, i.e. in some limiting case the catenoids with handle correspond to Scherk towers. Consider figure 8.12 for the notation. For a complete imbedded minimal surface with β_2^*, φ and β_1^* of the form $\frac{\pi}{k}$ with an integer k we must consider a three parameter problem. This is currently not possible. We can construct a surface with $\beta_1^* = \beta_2^* = \frac{\pi}{2}$: this is the Scherk tower discussed before. Let us discuss a solution with $\beta_1^* = \frac{\pi}{2}$ and $\varphi = \frac{\pi}{k}$, β_2^* will be arbitrary. This would give a catenoid with k horizontal handles along its waist, but the complete surface will generally not be embedded since β_2^* will be arbitrary.

Choose l_1 and l_2 small such that the situation exhibits Euclidean behavior. We use lemma 32 to estimate the sector angles. Let ϵ stand for arbitrarily small numbers. Then for fixed $\alpha_2(l_2)$ we can always choose $\alpha_1(l_1)=\frac{\pi}{2} + \epsilon$ to obtain $\beta_1 = \frac{\pi}{2}$. Choosing $\alpha_2(l_2)=\epsilon$, we obtain $\varphi = \frac{\pi}{2} - \epsilon$ and for $\alpha_2(l_2)=\frac{\pi}{2}$ we get $\varphi = \epsilon$. Therefore we have existence of pairs $\beta_1 = \frac{\pi}{2}$, $\varphi = \frac{\pi}{k}$ for each $k¿2$ by the intermediate value argument applied to φ_2. The continuity of α_2 comes from the ability to rotate the contours around l_2 in both directions, leaving the surface between both rotated copies.

In figure 8.13 we show a picture of a hyperbolic catenoid with handles.

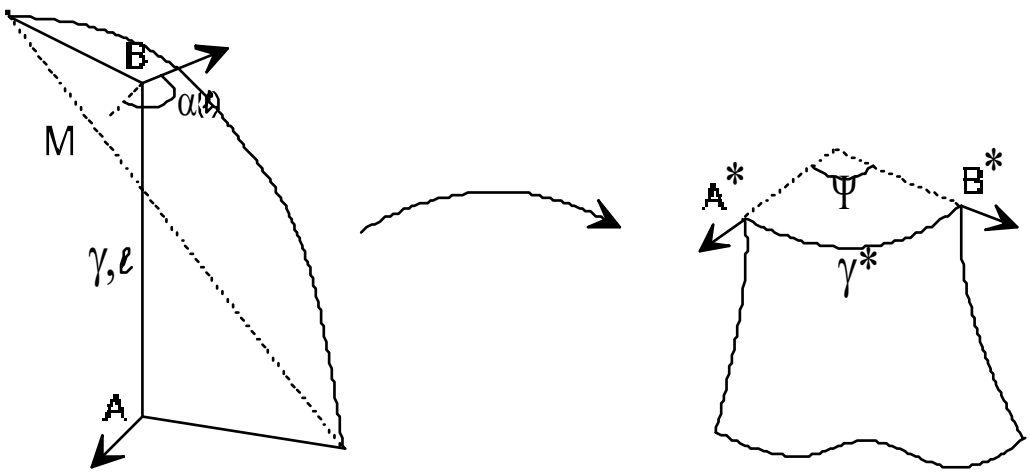

Figure 8.1: Standard Comparison with Helicoid

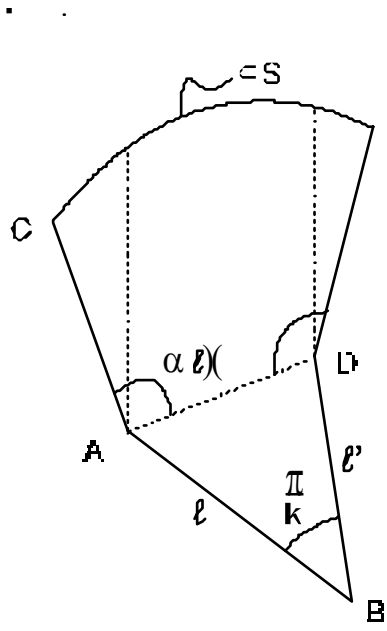

Figure 8.2: Conjugate Contour of Second Scherk Cousin

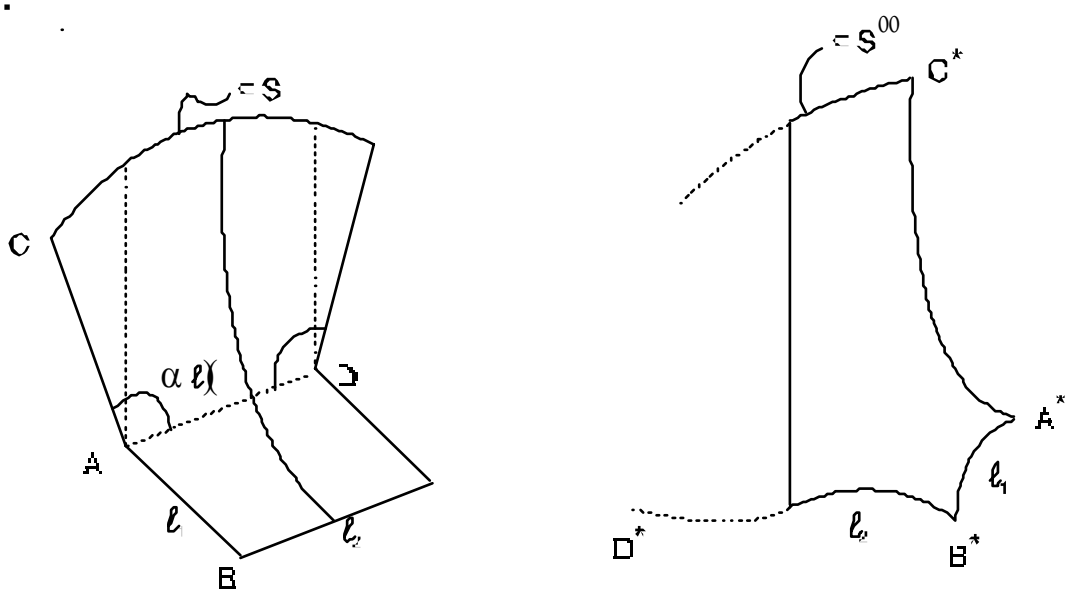

Figure 8.3: Conjugate Contour of First Scherk Cousin with Handle

Figure 8.4: Fundamental Piece of the Hyperbolic Scherk Surface with Handle

Figure 8.5: Hyperbolic Scherk Surface with Handle

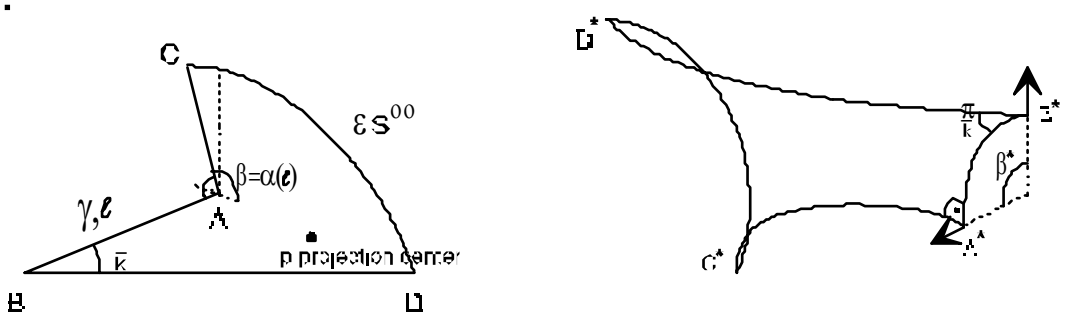

Figure 8.6: Conjugate Contour for Hyperbolic k-noids

.

Figure 8.7: Hyperbolic Trinoids with Different Ends

Figure 8.8: Hyperbolic Minimal Surface in a $60°-$Cube

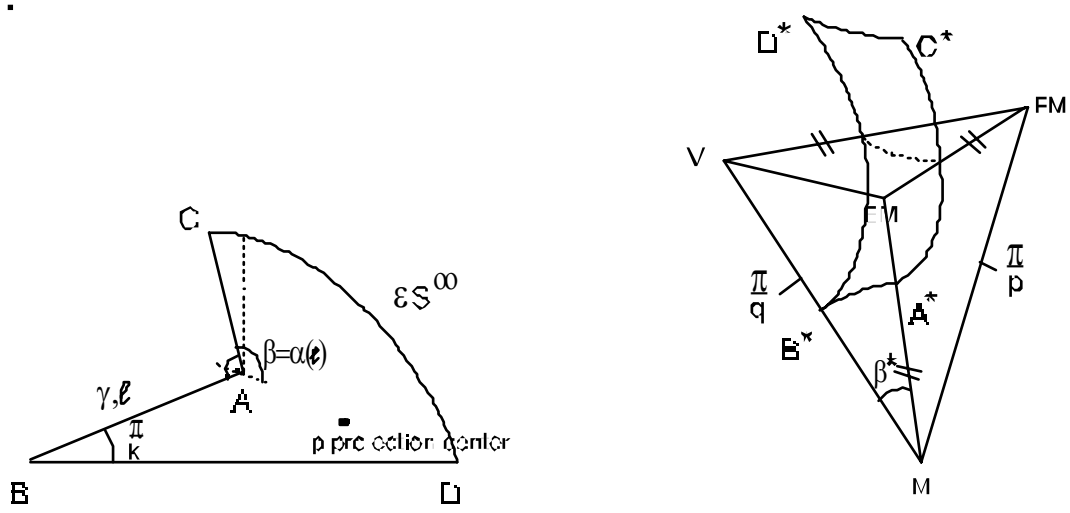

Figure 8.9: Conjugate Contour of Hyperbolic Platonoids

Figure 8.10: Hyperbolic Platonoid with Cubical Symmetry

Figure 8.11: Hyperbolic Platonoid with Dodecahedral Symmetry

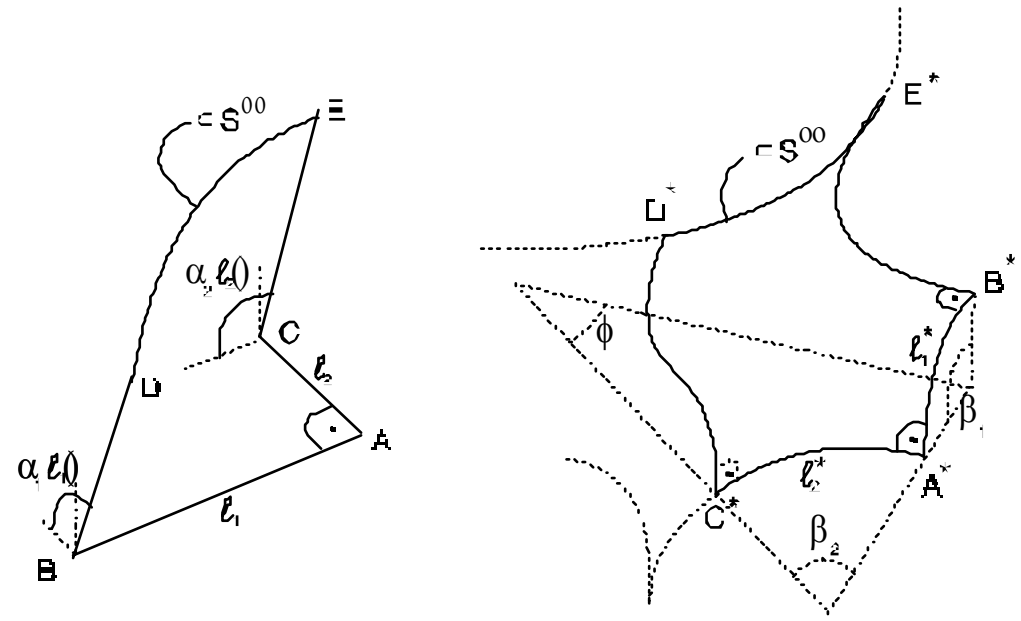

Figure 8.12: Contour for Hyperbolic Catenoid with Handle

.

Figure 8.13: Hyperbolic Catenoid with Handles

Chapter 9

Computation of Hyperbolic Minimal Surfaces

For the numerical computation of the minimal surfaces in this work we used a minimization algorithm developed by Pinkall and Polthier [27] for discrete surfaces in $\mathbf{R}^3$, S^3, and H^3. We will give a short overview of the general principles of this algorithm, but refer for all proofs, all related material and further details to [27].

9.1. The Minimization Algorithm

A discrete surface in a three dimensional space form is defined to be a topological simplicial complex consisting of triangles. For this definition and that of maps between such surfaces we use the embedding of the space form in a linear space as in chapter 1. Such a surface is then defined by its vertices, and the interior of each triangle is identical to the span of its three vertices w.r.t. the ambient vector space structure. Discrete surfaces are called area-minimizing iff small pertubations of a set of surface vertices would increase the total area. We now construct a minimizing sequence $\{M_i\}$ of discrete surface. In principle we fix the combinatorial type of the triangulation, but in practice we adaptivly refine the triangulation w.r.t. a discrete curvature function defined on the surface. For the algorithm we use the following minimization step:

Algorithm: Given a boundary contour Γ and a discrete surface M_i in $\mathrm{H}^3 \subset \mathbf{R}^4_L$ we compute the next surface M_{i+1} as the minimizer of the Dirichlet functional

$$M_{i+1} = \min_M \frac{1}{2} \int_{M_i} |\nabla(f : M_i \to M)|^2 ,$$

where f is piecewise linear on all triangles of M_i and M is of the same combinatorial type as M_i. Then use M_{i+1} as a domain and minimize again.

Pay attention to the fact that we do not use a planar two-dimensional domain but instead the most recent computed surface M_i. The used metric on M_i and in image space is the lorentzian metric in our case. Numerically we are left within

each step with a linear problem of computing the surface M_{i+1} where the minimum of the quadratic function is attained. This minimization method is faster than the other algorithms since it has no non-linear steps. During each step the area of the image surface is less than the area of the domain surface. Since we always step to the absolute minimum of the Dirichlet integral in each iteration and do not move along the area gradient we proceed discrete also in time direction.

9.2. Boundary Types

The algorithm respects different boundary types. A fixed boundary remains as it is during all minimization steps. A straight line, i.e. a hyperbolic geodesic being part of the boundary, indicates the algorithm that its boundary vertices may vary their position on the straight line. The third boundary type is a planar symmetry arc. In this case all boundary points may vary on the plane defined by the planar arc, therefore allowing the specification of free boundary value problems in hyperbolic space.

Handling boundary arcs in such different ways allows us to continue the minimized surfaces as discrete minimal surfaces along their boundary symmetry arcs by reflection. Such a continued surface will also be minimal along the reflection line.

In the two example sessions the infinite part of the initial surfaces were set to be fixed. The finite boundary parts of the examples whose existence proof uses the conjugate surface construction are generally symmetry arcs restricted to planes, i.e. free boundary value problems. Since we computed the minimum of the area, fundamental parts of these surfaces are therefore stable. This has to be seen in contrast to the fact, that in general the conjugate of a minimizing surface need not be minimizing again, it may be an instable minimal surface.

References

[1] M.T. Anderson, *Complete Minimal Hypersurfaces in Hyperbolic n-Manifolds*, Comm. Math. Helv. **58** (1983), 264-290.

[2] M.T. Anderson, *Complete Minimal Varietes in Hyperbolic Space*, Invent. math. **69** (1982), 477-494.

[3] A.F. Beardon, *The Geometry of Discrete Groups*, Springer Verlag 1983.

[4] M.P. Do Carmo, M. Dajczer, *Rotation Hypersurfaces in Spaces of Constant Curvature*, Trans. of the AMS **277.2** (1983), 685-709.

[5] U. Dierkes, S. Hildebrandt, A. Küster, O. Wohlrab, *Minimal Surfaces I + II*, Grundlehren Math. Wiss. **295**, Springer Verlag 1992.

[6] J. Douglas, *Solution of the Problem of Plateau*, Trans. Amer. Math. Soc. **33** (1931), 263-321.

[7] J.H. Eschenburg, *Maximumprinciple for Hypersurfaces*, Manuscr. Math. **64** (1989), 55-75.

[8] D. Gilbarg, N.S. Trudinger, *Elliptic Partial Differential Equations of Second Order*, Grundlehren math. Wiss. **224**, Springer Verlag Second Edition 1983.

[9] R.D. Gulliver, *Regularity of Minimizing Surfaces of Prescribed Mean Curvature*, Ann. of. Math. **97** (1973), 275-305.

[10] R. Hardt, F.H. Lin, *Regularity at Infinity for Area-Minimizing Hypersurfaces in Hyperbolic Space*, Invent. Math. **88** (1987), 217-224.

[11] E. Heinz, S. Hildebrandt, *Some Remarks on Minimal Surfaces in Riemannian Manifolds*, Comm. Pure Appl. Math. **23** (1970), 371-377.

[12] H. Jenkins, J. Serrin, *Variational Problems of Minimal Surface Type, II. Boundary Value Problems for the Minimal Surface Equation*, Arch. Ration. Mech. Anal. **21** (1965/66), 321-342.

[13] L.P.M. Jorge, W.H. Meeks, *The Topology of Complete Minimal Surfaces of Finite Total Gauß Curvature*, Topology **22** (1983), 203-221.

[14] H. Karcher, *Embedded Minimal Surfaces Derived from Scherk's examples*, Manuscr. Math. **62** (1988), 83-114.

[15] H. Karcher, *Triply Periodic Minimal Surfaces of Alan Schoen and Their Constant Mean Curvature Companions*, Manuscr. Math. **64** (1989), 291-357.

[16] H. Karcher, *Construction of Higher Genus Embedded Minimal Surfaces*, Geom. and Top. of Sub. III World Sc. (1990), 174-191

[17] H. Karcher, *Construction of Minimal Surfaces*. In: Surveys in Geometry 1989/90, University of Tokyo 1989.

[18] H. Karcher, U. Pinkall, I. Sterling, *New Minimal Surfaces in S^3*, J. Diff. Geom. **28** (1988), 169-185.

[19] H.B. Lawson, *Complete Minimal Surfaces in S^3*, Ann. of Math. **92** (1970), 335-374.

[20] H.B. Lawson, *The Global Behavior of Minimal Surfaces in S^3*, Ann. of Math. **92** (1970), 224-237.

[21] G. Levitt, H. Rosenberg, *Symmetry of Constant Mean Curvature Hypersurfaces in Hyperbolic Space*, Duke Math. J. **52.1** (1985), 53-59.

[22] F.H. Lin, *On the Dirichlet Problem for Minimal Graphs in Hyperbolic Space*, Invent. Math. **96** (1989), 593-612.

[23] A. Lonseth, *The Problem of Plateau in Hyperbolic Space*, Amer. J. Math. **64** (1942), 229-259.

[24] H. Mori, *Minimal Surfaces of Revolution in H^3 and Their Global Stability*, Idiana Univ. Math. J. **30.5** (1981), 787-794.

[25] C.B. Morrey, *Multiple Integrals in the Calculus of Variations*, Grundlehren math. Wiss. **130,** Springer Verlag 1966.

[26] J.C.C Nitsche, *Vorlesungen über Minimalflächen*, Grundlehren math. Wiss. **199**, Springer Verlag 1975.

[27] U. Pinkall, K. Polthier, *Computing Discrete Minimal Surfaces and Their Conjugates*, J. Experimental Math., to appear.

[28] K. Polthier, *Neue Minimalflächen in H^3*, Sonderforschungsbereich 256, Bonn, Report **7** (1989).

[29] K. Polthier, *New Periodic Minimal Surfaces in H^3*, Proc. Centr. Math. Anal., Canberra, **26** (1991), 201-210.

[30] K. Polthier, *Geometric Data for Triply Periodic Minimal Surfaces in Spaces of Constant Curvature*. In: Geometric Analysis and Computer Graphics (P. Concus, D. Hoffman, R. Finn, Eds.). Springer Verlag 1991, pp. 141-145.

[31] T. Rado, *The Problem of Least Area and the Problem of Plateau*, Math. Z. **32** (1930), 763-796.

[32] C.S. Schefel, *Compactness of Saddle Surfaces*, Sib. Math. J. **8.3** (1967) 705-714 (russian).

[33] H.A. Schwarz, *Gesammelte Mathematische Abhandlungen*, Springer Verlag, Berlin 1890.

[34] B. Smyth, *Stationary Minimal Surfaces with Boundary on a Simplex*, Invent. Math. **76** (1984), 411-420.

[35] K. Uhlenbeck, *Closed Minimal Surfaces in Hyperbolic 3-Manifolds*. In: Seminar on Minimal Submanifolds, Ann. Math. Stud. **103** Princeton 1983, 147-168.